

On the ~~Role~~ origin of Westerly Wind Anomalies in the Development of western equatorial Pacific sea level anomaly prior to the ~~the~~ 1982-1983 El Niño

David J. Webb

National Oceanography Centre, Southampton SO14 3ZH, U.K.

Correspondence: D.J.Webb (djw@noc.ac.uk)

Abstract.

A recent study of two strong El Niños highlighted the potential importance of a region of low sea level that developed in the western equatorial Pacific prior to the classic east Pacific El Niños of 1982-1983 and 1997-1998. Here the cause of the low sea level in 1982 is investigated using a series of runs of a global ocean model with different wind fields and initial conditions.

5 The results indicate that the low sea level was due to the increased wind shear that developed in the western Pacific just north of the Equator during 1982. This generated Ekman divergence at the latitudes of the North Equatorial Trough, raising the underlying density surfaces and increasing the depth of the trough. This also in turn increased the strength of the North Equatorial Counter Current which lies on the southern slope of the trough.

10 The anomalous westerly winds associated with Madden-Julian Madden-Julian Oscillations are often held responsible for triggering El Niños through the generation of westerly wind bursts and the resulting equatorial Kelvin waves in the ocean.

However if Webb (2018b) is correct, the present results imply that support a different physical process was involved in which Ekman divergence due to the same winds, increased the heat transported mechanism in which westerlies in the western Pacific, possibly MJO related, cause strong El Niños through Ekman pumping at the latitude of the North Equatorial Trough and the resulting increased eastward transport of Warm Pool water by the North Equatorial Counter Current~~early in the year and ultimately caused the strong 1982-1983 El Niño.~~

Copyright statement. The works published in this journal are distributed under the Creative Commons Attribution 4.0 License. This licence does not affect this Crown copyright work, which is re-usable under the Open Government Licence (OGL). The Creative Commons Attribution 4.0 License and the OGL are interoperable and do not conflict with, reduce or limit each other.

1 Introduction

20 ~~When Wyrtki (1973, 1974a) studied tide gauge data from The North Equatorial Countercurrent (NECC) flows from west to east across the Pacific at latitudes between 5°N and 10°N. The total transport is in the range 10-30 Sv, making it comparable with the major northern hemisphere currents (Knauss, 1961; Wyrtki, 1974a,b; Johnson et al., 2002).~~

Physically it is a geostrophic current lying between the sea level minimum of the ~~equatorial Pacific~~, he found that the strong (or classic) El Niños were correlated with increased differences in sea-level across the North Equatorial Counter Current 25 (NECC). As such sea level differences are balanced by geostrophic currents, the increased difference implied that the NECC was stronger during an El Niño and so would carry more warm water than normal Trough and the sea level maximum of the North Equatorial Ridge (Sverdrup, 1947; Neumann and Pierson, 1966). However it is also a shallow current with a depth of only two to three hundred metres, the north-south pressure differences near the surface being balanced by large north-south gradients in the near surface density surfaces (Wyrtki and Kilonsky, 1984; Taft and Kovala, 1981, 1982; Bryden and Brady, 1985).

30

The current is important because it carries warm water eastwards out of the ~~western Pacific warm pool across to the eastern side of the ocean. He hypothesised that it was this increased transport which ultimately caused the large scale changes in atmospheric circulation~~ west Pacific Warm Pool (Johnson et al., 2002). It is also unusual in that it flows in the opposite direction to the steady trade winds of the North Pacific. Montgomery and Palmen (1940) originally suggested that the current flowed 35 downhill from west to east across the Pacific but, using geostrophic theory, Sverdrup (1947) showed that it was the result of the shear in the wind field at latitudes near the Inter-Tropical Convergence Zone (ITCZ) (See also Munk, 1950). The current also lies in a region where the inverse of the Coriolis term is a rapidly changing function of latitude. As a result small changes in the position of the trough can have a significant effect on the velocity of the current.

For reasons that are not understood this hypothesis was not developed further, but recently Webb (2018b), in an analysis of 40 results from a high resolution run of the Nemo global ocean model, concluded that changes in sea level and changes the ~~Early~~ studies of the current were limited by lack of data but, using data from bathythermographs, Myers (1979) showed that the depth of the North Equatorial Trough had a significant annual signal, which he identified as being due to an annual Rossby wave.

Further developments in ocean instrumentation have provided more information on the NECC, satellite observations of sea 45 surface temperature (SST) showing tropical instability eddies (often called waves: Hansen and Paul, 1984; Chelton et al., 2000; Kennan and both warm the Equatorial Current and cool the NECC (Menkes et al., 2006; Jochum et al., 2007), the effect possibly being least in El Niño years (Yu and Liu, 2003).

Satellite altimeter measurements of sea level have errors of only a few centimetres and, as the North Equatorial Trough has a depth of order one metre, this allows the annual and interannual changes of both the trough and the NECC to be studied in detail (Zhao et al., 2013; Tan and Zhou, 2018).

50 1.1 Connection with the El Niño

Originally El Niño was the name of a southward flowing current off the coast of Peru which affected fisheries (Wyrtki et al., 1976; Philander However the studies reported in Love (1972, 1975) and Wyrtki et al. (1976) connected it to the very large changes in surface 55 temperature and thermocline depth observed in the nearby East Pacific Cold Pool.

Wyrtki (1973) was the first to make the further connection between this oceanographic El Niño and the strength of the NECC in the western Pacific, ~~near 6° N, were key precursors to the development of the strong El Niños of 1982–1983 and 1997–1998. He also suggested that the NECC might trigger an El Niño by transporting West Pacific Warm Pool water to the east.~~

Webb (2018b) identified other mechanisms that appeared to aid the development of the El Niño. Myers and Donguy (1984) then showed that the NECC transport increased by between 25% and 50% while the strong 1982-83 El Niño, but these only started operating once was developing. They also found that the total transport of warm water ($>28^{\circ}\text{C}$) by the NECC was consistent with their estimate of the loss of warm water from the west Pacific warm pool had started moving eastwards. Thus the lowering of sea level in western West Pacific Warm Pool.

Although Wyrtki's hypothesis was not developed further, his work complimented the study by Bjerknes (1969) which showed a correlation between water temperatures in the equatorial Pacific and the resulting increase in the strength of the NECC appeared to be critical factors Southern Oscillation (Philander, 1985). This led to further uses of the term El Niño to describe both its world wide influence and the air-sea interaction (or mechanism) behind the event (Cane, 2011).

Bjerknes (1969) also argued that the east-west temperature gradient along the Equator was involved and this is usually taken to imply that the temperature of the East Pacific Cold Pool is a key part of the El Niño mechanism. However Clarke (2014) doubts this, because the east Pacific winds are only weakly affected by an El Niño. If he is correct, temperature changes in the Cold Pool are a consequence of and not a cause of El Niños.

The NECC flows along the southern boundary of the North Pacific Trough, a region of low sea level which extends from east to west across the equatorial Pacific. In the west Pacific, the trough lies roughly between latitudes 4° N and 12° N . In the east Pacific it lies further north, typically between 6° N and 14° N . Further studies showed that Bjerknes' correlation was strongest when using ocean temperatures from the central Pacific. As a result most modern studies of the Southern Oscillation use the Nino 3.4 index to measure the strength of an El Niño (Larkin and Harrison, 2005). This is based on the mean sea surface temperature in the central Pacific between 170°W and 120°W , and between 5°S and 5°N .

To the south of the trough lies the equatorial Ridge. When the Equatorial Current is flowing this has a maxima just to As well as affecting surface winds in the western and central Pacific, the atmospheric El Niño requires the centre of deep atmospheric convection to move from the maritime continent and the north and south of the equator and a small minimum of sea level along the equator. During periods when the current is zero or reverses there is a single maximum western Pacific into the central Pacific. Evans and Webster (2014), following Gadgil et al. (1984) and Zhang (1993), confirmed that this requires sea surface temperatures of 28°C and above during wet seasons and even higher temperatures during dry periods.

In the central Pacific, such temperatures are found on the Equator. This behaviour reflects the fact that although the vertical component of the Coriolis vector is zero during an El Niño, but eastern Pacific equatorial temperatures never reach this value (Philander, 1985, Fig. 2). Instead the eastward limit of warm water on the Equator, on average the Equatorial current north and south of the equator is in balance with the slope in sea level is closely correlated with the Southern Oscillation Index (Picaut et al., 1996).

In the eastern Pacific, temperatures sufficient to trigger deep atmospheric convection are often found further north in the ocean off Central America and along the path of the NECC close to the ITCZ.

This balance also holds for the NECC, the transport at each latitude depending on both the Coriolis vector there Meteorological studies also showed that the start of an El Niño was often connected with one or more Madden-Julian Oscillations (MJOs) (Madden and Julian, 1971, 1972). In his review, Zhang (2005) describes MJOs as individual events with lifetimes of between

30 and the local gradient of sea level between the Equatorial Ridge and the 100 days and with the property that there is never more than one major event in existence at a time. Each one consists of an area, spanning the Equator, in which there is an increased density of short lived convective cloud groups.

95 The events progress eastwards at speeds around 5 ms^{-1} , starting in the western Indian Ocean and dying out after passing the western Pacific. At sea level they are associated with inflowing winds from the east and west, but in the Pacific the westerly winds may extend past the centre of the North Pacific Trough cloud groups.

Early each year, annual changes in the wind field

1.2 El Niño models and theories

100 Following Wyrtki and Bjerknes, most theoretical studies of the ocean's contribution to El Niño have focussed on the Cold Pool. This is a narrow band of low sea surface temperatures, centred on the Equator in the eastern Pacific increase the Ekman transport of water out of the trough. This lowers sea level in the eastern trough and generates annual Rossby waves which propagate the region of low sea level to the west. The speed of the waves depends on latitude, the wave at 6° N affecting sea level at 180° E in late May. At 9° N the annual wave is less well defined. When clearly present it only reaches 210° E (150° W) by late May. During a normal year this is a result of the wind generated upwelling of cold water from depths of around 200m, but during an El Niño the surface thermocline becomes thicker and less cold water is upwelled.

105 In a normal year, the Rossby waves also tend to decay as they move westwards, so that the wave at 6° N has little effect beyond 180° E . However Webb (2018b) found that, in 1982 and 1997, the wave appeared to continue into the far western Pacific. This had the effect of increasing the strength of Early theoretical studies, using analytic models or numerical models with a few layers (Hurlburt et al., 1976; McCreary, 1976, 1985; McPhaden, 1981, 1993), showed that the changes in the Cold Pool could be generated by wind variations in the western and central Pacific. This occurred via the propagation of baroclinic Kelvin waves in the equatorial wave guide. The studies also showed that only winds close to the equator were responsible (McCreary, 1976) and that off equatorial currents, such as the NECC, were not connected with the El Niño changes to the Cold Pool.

115 With the development of computer power, it was eventually possible to run ocean models with much more detailed physics and with enough horizontal and vertical resolution to resolve the key currents and structure of the ocean (Bryan, 1969; Semtner, 1974; Philander, 1989). The versions developed by Cox (1989), Madec et al. (1998) and Griffies et al. (2005) have been widely used in stand-alone mode and, coupled to an atmospheric model, for studies of climate.

120 Unfortunately the NECC can be poorly represented in such models (Lengaigne et al., 2002; Sun et al., 2019). Yu et al. (2000) investigated the forcing of ocean only models and showed that this was a result of the atmospheric reanalysis datasets underestimating the curl of the wind field near the latitudes of the ITCZ (Byrne et al., 2018), and overestimating the strength of easterly winds on the Equator.

125 The study also found that, of the datasets studied, the ECMWF reanalysis was best at generating a realistic NECC. This may be because the ECMWF model was using a spherical harmonic expansion which requires less smoothing than normal finite difference schemes to overcome non-linear instabilities.

There is a related problem with coupled ocean-atmosphere models which fail to generate realistic El Niños (Guilyardi et al., 2009; Ham a
This again may be due to the limited resolution of the atmospheric component being insufficient to accurately represent features
such as the ITCZ.

Further studies using observational data have indicated that there are two types of El Niño (Larkin and Harrison, 2005; Ashok et al., 2007
130 The most common are the central Pacific (CP) or Modoki events, in which the centre of atmospheric convection moves to the
NECC in the region and significantly increasing the transport of warm water out of the Western Pacific Warm Pool to wards the
central Pacific. As argued by Webb (2018b), this was the start of a series of processes which eventually moved deep atmospheric
convection to the eastern Pacific, so causing the strong More rarely the centre of convection moves even further east to give
the strong eastern Pacific (EP) El Niños. These behave like the classic El Niños of 1982-1983 and 1997-98 (Philander, 1985),
135 which Wyrtki (1974a) proposed were triggered by the NECC.

If the increased strength of the NECC is responsible for triggering strong

1.3 Wyrtki's hypothesis

Although neglected for many years, Wyrtki's hypothesis is supported by more recent studies using altimeter data (Zhang and Busalacchi, 19
These confirm the increased transport by the NECC during EP El Niños, then it becomes important to understand precisely
140 why the sea level dropped in the way observed. Zhao et al. (2013) showing that the increased transport in the western Pacific
occurs before the corresponding change in the Nino 3.4 index. They thus leave open the possibility that the increased transport
has a role in triggering subsequent EP El Niños, rather than being part of the ocean's response to the event. The studies also
show that there are changes in the NECC during CP El Niños, indicating that both types of El Niño may be affected by the
NECC in the western Pacific

145 Because the timing coincided with the arrival of the annual Rossby wave, Webb (2018b) supposed that the Rossby wave was
responsible. However in both 1982 and 1997 the strength of the annual wave at 6° N in the central Pacific was little different
from other years, but it is possible that the propagation of the wave further west was due to changes in ocean stratification.

Such changes might focus the wave energy nearer the surface of the ocean. Alternatively horizontal focusing may also have
increased the amplitude of the wave. Further support for the hypothesis comes from Webb (2018b) who used results from a high
150 resolution global ocean model to study the ocean during the strong EP El Niños of 1982-1983 and 1997-1998.

But the annual Rossby wave may not be involved. Other possibilities include sea level changes in the Indian Ocean
affecting the western Pacific or changes in the Indonesian Throughflow which involve sea level. There is also atmospheric
forcing, possibly changes due to the local winds or changes elsewhere which affect sea level in the region. The model used by
Webb (2018b) was forced by modified ECMWF reanalysis fields (Dussin et al., 2016) and produced sea level and sea surface
155 temperature fields in the equatorial Pacific in close agreement with satellite observations (Webb et al., 2020). The results
indicate that the modified ECMWF reanalysis fields accurately represented the wind stress curl and so generated a realistic
NECC.

Unlike previous studies, Webb (2018b) concentrated on water with temperatures above 28°C, sufficient to trigger deep atmospheric convection. The study showed that, while the strong El Niños were developing, the NECC carried warm water into the eastern Pacific far in advance of water with similar temperatures on the Equator.

There is also the possibility that the model itself may be faulty. However the model has been compared with observations in Webb (2016), which concentrated on the Pacific NINO regions and in Webb et al. (2020) which was a focussed study of the processes identified in Webb (2018b). Together the results mean that the drop cannot be easily explained as being due to an artifact of the model. The study also helped explain why the NECC does not carry Warm Pool water into the eastern Pacific every year, by showing that in normal years tropical instability waves mix in cold upwelled water from near the Equator and that this rapidly reduces temperatures in the NECC (See: Baturin and Niiler, 1997). In El Niño years the eddies are weaker so their effect on the NECC is reduced.

It also found that the start time of strong El Niño events resulted in warm water reaching the central and eastern Pacific at a time of year when the annual Rossby wave meant that the NECC was strongest there. This resulted in the warm water arriving off South America around the end of the year, thus providing a physical mechanism to explain the name originally given to classic EP El Niños.

1.4 Aims

Webb (2018b) also found that the drop in Finally the study showed that both the strong 1982-83 and 1997-98 El Niño events started when the depth of the western section of the North Equatorial Trough was unusually low. As a result the NECC transport, and the flux of Warm Pool water eastwards, were both much stronger than usual.

1.4 Low sea levels in the western Pacific

Webb (2018b) suggested that the low sea level in the western Pacific coincided with the arrival of the annual Rossby wave at 6° N. Initially it appeared that the drop may be trough was due to an increased amplitude of the Rossby wave in years when a strong unusually strong annual Rossby wave prior to each El Niño developed, but further analysis has shown that in such years the wave was. However further investigation showed that this is unlikely, as in each case the wave is not unusually large when it crossed as it crosses the central Pacific.

Another possible explanation is that the stratification in the Pacific, prior to an El Niño, is sufficient to focus the annual Rossby wave and so cause the region of lower than normal sea level levels. Alternatively the low sea level may not be connected with the annual Rossby wave and due to the Rossby wave but instead is due to some other process associated with the wind field. This could be a local feature occurring at or just before the period when sea level drops. Alternatively it could It could also be a response to forcing elsewhere in the ocean which, like the Rossby waves, which later propagates into the western Pacific.

To help clarify the cause of the drop in sea level, this paper reports on series of short ocean model runs, which focus the changes sea level which focus on changes in the western Pacific prior to the 1982-1983 El Niño. The model used is a 1/4° study uses an updated version of the Occam global ocean model based on the original Ocean model (de Cuevas et al., 1999) (Webb et al., 1997; de

In each run, the model is initialised from one of the archive datasets from the original run of the Nemo model and forced with ocean surface stresses calculated during the same run.

1.5 Structure of the report

In the first part of the paper, section 2 describes the model being used and how the model fields and forcing were converted from the 1/12~~degree~~ Nemo run to the grid of the $^{\circ}$ Nemo grid to the 1/4~~degree~~ model $^{\circ}$ Occam grid.

195 Section 3 then describes two tests carried out to validate the lower resolution model. In these the model was started from the Nemo archive datasets from early January 1981 and 1982 and then run for a year using the surface wind stresses from the same year. The resulting model fields were compared with the results from the original Nemo run.

200 The second part of the paper is concerned with a series of ~~further~~ runs of the Occam model with different wind fields. In this, ~~seection~~ Section 4 reports on two runs where the model was again ~~stated~~ started from early January 1981 and 1982, but with the wind forcing ~~is~~ from the opposite year. The results show that the main changes in sea level depend primarily on the wind field and, to first order, are independent of the stratification at the start of the run.

205 In section 5, ~~the test using the test that used the~~ 1982 initial conditions with 1981 winds, is repeated but starting later in the year when the annual Rossby wave has developed and is starting to cross the central Pacific. This is done as a check to see if some property of the Rossby wave is responsible for the sea level drop in the western Pacific. The results are similar to the earlier test, indicating that the wind generated Rossby wave is not responsible for the drop in sea level.

Section 6 takes the study further with a run designed to investigate whether the winds causing the drop in sea level are local to the western equatorial Pacific or propagate in from other parts of the ocean. The results show that it is the local winds that are responsible.

210 This leads to the final part of the paper where ~~in Seection~~, in section 7, a study is made of the Ekman pumping in the western Equatorial Pacific due to the local winds. This concludes that the drop of sea level in the model runs is consistent with an enhanced level of Ekman suction that occurred north of the Equator during the first half of 1982.

The final section discusses these results and how they affect our understanding of how and why strong El ~~Nin~~ \circ s-Ni \circ ns develop.

215 2 The Occam 1/4 $^{\circ}$ global ocean model

~~The study reported here makes use of a recent version of the Occam global ocean model (Webb et al., 1997; de Cuevas et al., 1999).~~
~~Occam~~ Occam is a primitive equation model, based on the Bryan-Cox-Semtner series of models (Bryan, 1969; Cox, 1989; Semtner, 1974).

220 It uses a regular latitude-longitude grid for all the oceans except the North Atlantic and Arctic. For the latter ~~basins~~ it uses a second rotated latitude-longitude grid which is matched to the first grid at the Equator. The Bering Strait between the Arctic and the North Pacific is ~~modeled~~ modelled with a simple channel model.

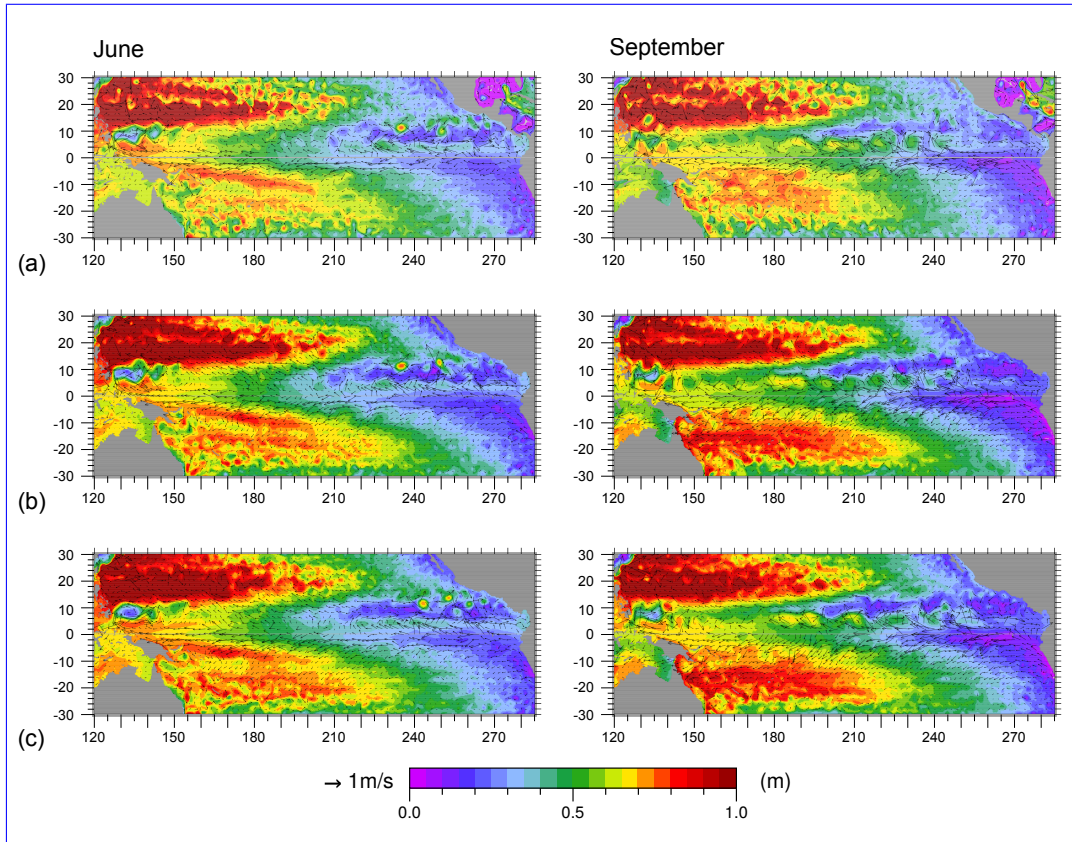


Figure 1. Sea level (m) plus surface currents on the 6th June and 9th September for (a) Nemo in 1981, (b) Occam in 1981, started January 1981 (c) Occam in 1982, started January 1982 but with 1981 winds.

This version of Occam has Occam uses 1/4 degree resolution in both longitude and latitude. In the vertical it has 66 levels, instead of the 75 levels of the Nemo run, and makes use of an existing global topography has previously been that was checked against a database of critical oceanographic sills (Thompson, 1996). Both models use the Occam and Nemo models have 225 increased vertical resolution in the surface layers, Occam using 24 layers in the top 300m and Nemo 34 layers, the difference being primarily due to Nemo's extra resolution in the top 100m.

Occam uses harmonic mixing in the horizontal and the scheme of Pacanowski and Philander (1981) for vertical mixing. For horizontal advection it uses the second order split-quick scheme (Webb et al., 1998) for both momentum and tracers. For vertical advection the vertical advection of momentum it uses the scheme of Webb (1995).

Occam was chosen for these tests primarily because of its computational efficiency and because the amount of computer time available was limited. The efficiency arises partly because, unlike Nemo, it uses a regular grid and partly because the code includes fewer of the complex physical options included in Nemo.

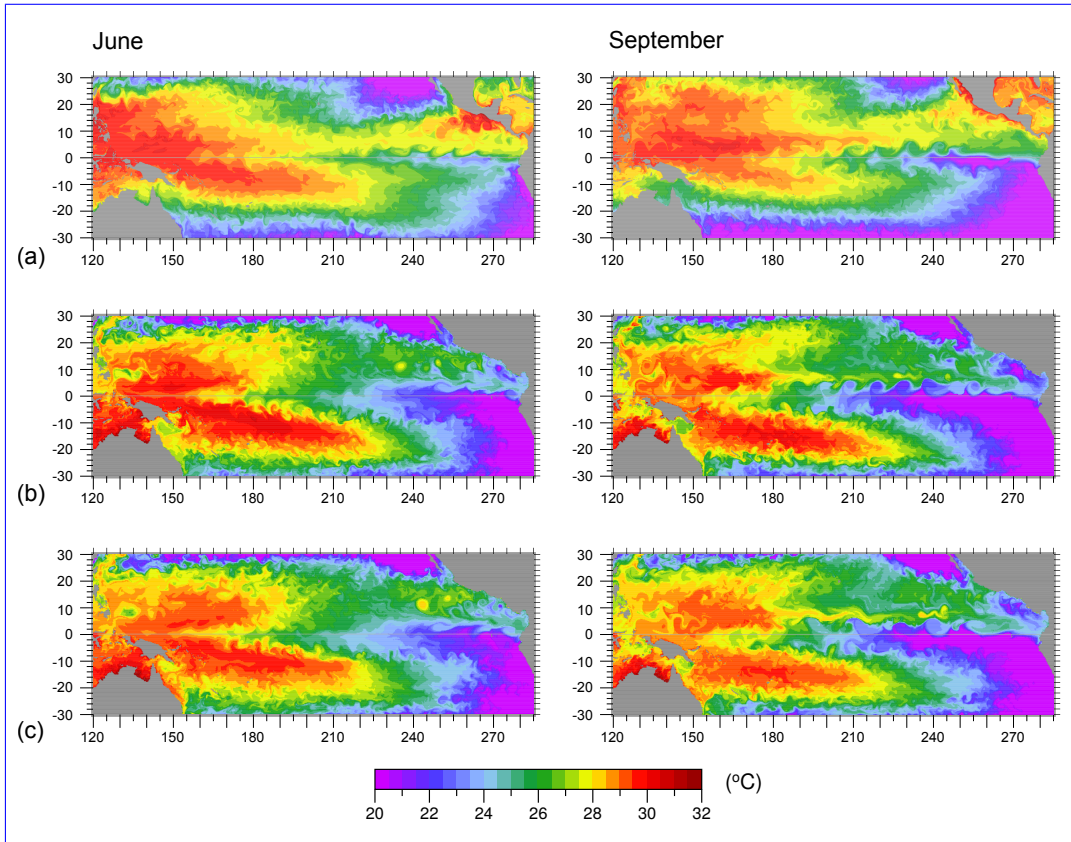


Figure 2. Surface temperature ($^{\circ}\text{C}$) on the 6th June and 9th September for (a) Nemo in 1981, (b) Occam in 1981, started January 1981 (c) Occam in 1982, started January 1982 but with 1981 winds.

However most ocean models are limited not by the speed of the processor but by the ~~lengthy~~ length of time needed to transfer data from main memory. Occam's main advantage is that it overcomes this by vectorising the code in the vertical¹.

235 2.1 Initialisation and forcing

The model runs reported here were initialised by averaging the archived data from the high-resolution Nemo model onto the Occam grid. Variable values within each Occam ocean cell were calculated by averaging over the intersection of the Occam and Nemo cells. In the case of vector quantities, vectors were rotated to the Occam grid before averaging.

240 The runs were also carried out with zero flux of heat and salt across the ocean surface. Each run is ~~only for~~ for ~~only~~ a few months and, although the surface temperatures and salinities are affected, this approximation allows the analysis to concentrate on the effects of ~~the~~ wind stress and of advection and diffusion within the ocean.

¹This means that all the variables needed to time step the cells in a vertical column are held in high speed cache at the same time and no extra references to main memory are required. Also when moving from one column of ocean cells to the next, most of the data required is already in cache.

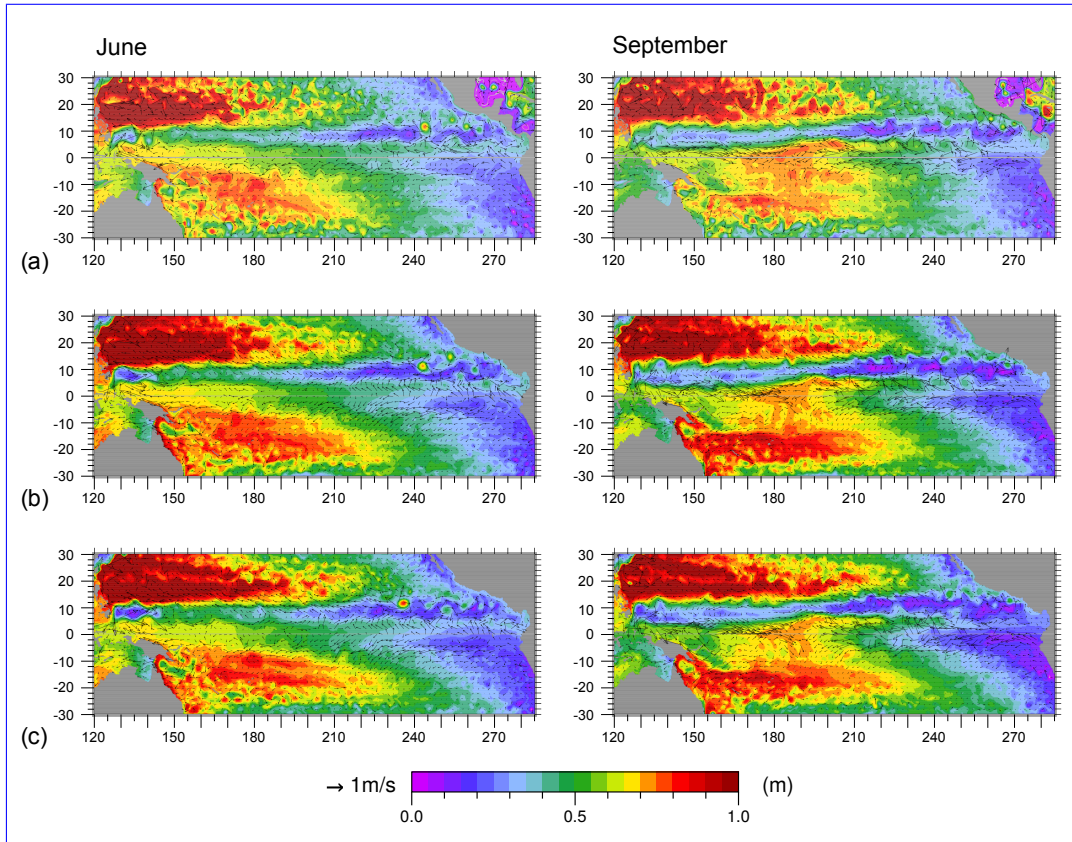


Figure 3. Sea level (m) plus surface currents on the 6th June and 9th September for (a) Nemo in 1982, (b) Occam in 1982, started January 1982 (c) Occam in 1981, started January 1981 but with 1982 winds.

Each Nemo archive datasets contain the ocean and forcing fields averaged over the previous 5 days. Thus when initialising the Occam model and when specifying the wind forcing, the time of each Nemo dataset is set to the central time of the averaging period. However when specifying particular Nemo archive files, the original archive date is used.

245 The use of five day averages filters out ~~all the high~~ ~~higher~~ frequency components of the wind field and also means that the ocean state used to initialise the Occam model may be unusually smooth. The resulting lack of high frequency oscillations may affect vertical mixing in the ocean but should otherwise have little effect on lower frequency variations in sea level and current velocity, which are the focus of this study.

3 Validation

250 ~~The use of the Oceam 1/4 degree model for short runs~~ Previously the Occam model has been widely used for successful oceanographic research but here the use of Occam with the modified forcing from the Nemo archive was validated by compar-

ing the model results over a full year with the results from the Nemo 1/12~~degree run~~ $^{\circ}$ run. The latter was validated against observations by Webb et al. (2020).

For the two cases reported here, the model Two runs of the Occam model are considered. In the first, designed to check performance in a normal year, Occam was initialised from the Nemo archive datasets made on from the 5th January 1981 and 1981. In the second, a test of a strong El Niño year, the model was started from the 5th January 1982. The run was Both runs were then continued for a full year, using the Nemo archived winds surface wind stresses from that year.

3.1 Comparison of 1981 results

This paper is primarily concerned with the behaviour of sea level along 6° N in the Pacific. Fig. ?? compares the Oceam model sea levels at this latitude with the 1981 sea levels of the full Nemo run. In Fig. 1, the top two pairs of figures show sea level from the Nemo and Occam models on the 6th June and the 9th September 1981. The 6th June is chosen because the corresponding date in 1982 can be used to check the early deepening of the North Equatorial Trough in the western Pacific that occurs prior to the 1982-1983 El Niño. Similarly the 9th September is chosen as a check on how well Occam reproduces the increased depth of the trough, and corresponding increased strength of the NECC, across the whole of the Pacific, during the autumn months.

The figure shows that the response of the two models is similar, both models showing At the largest scales the Occam model is in close agreement with Nemo, the main differences arising from slightly more extreme maxima and minima. Thus in September, maximum sea level in the South Pacific Gyre is slightly higher in Occam. Similarly the minimum sea levels in the Cold Pool on the Equator and within the North Equatorial Trough are slightly lower.

This paper is primarily concerned with the behaviour of the NECC and the associated sea levels in the North Equatorial Trough. Here Occam shows a similar westward propagation of the trough during the year and a similar growth of the ridge on the southern side of the NECC. The September figures also show a similar development in Occam of the short wavelength features due to on the ridge, associated with the growth of tropical instability eddies and both showing a similar annual Rossby wave. This arrives in the western Pacific just after mid-year, but in both cases there is only a reasonably small drop.

In June, both Nemo and Occam show that the trough is particularly weak in the central Pacific resulting in an almost non-existent NECC. However in September, with a greater contrast between ridge and trough, both models show a stronger NECC.

At the western ends of the trough and ridge, Occam shows a similar development of the high and low sea level regions associated with both the Halmahera and Mindinai eddies (Kashino et al., 2003) and the initial meanders of the NECC. In September these decay in amplitude, in contrast to the growth of the trough and ridge features seen in the central and eastern Pacific.

The development of sea level during the year at 6° N in both Nemo and Occam is shown in panels (a) and (c) of Fig. 5. The average slope in sea level in the far western Pacific Occam matches that of Nemo and in the central and eastern Pacific, Occam shows a similar development of the ridges due to the growth and propagation of tropical instability eddies. The figure also shows the low sea levels due to the propagation on the annual Rossby wave at 6° N. This starts in the eastern Pacific early in the year and reaches the dateline in July and August.

Fig. ?? compares sea levels along the equator. Again there is reasonable agreement, both figures showing equatorial Kelvin waves of similar strength and both showing similar variations in sea level in the far west.

Figs. ?? to ??, compare the surface temperature and sea level fields from the two models around the 4th June and 2nd September 1981. In both sets of temperature figures, The corresponding sea levels on the Equator are shown in panels (a) and (c) of Fig. 3.3. Again the overall east-west slope is similar and Occam reproduces the eastward propagating equatorial waves that can be generated by westerly wind bursts in the Oceam model tends to be warmer than Nemo western equatorial Pacific. There are differences between the two model runs but in both models sea level is a maximum either close to the western boundary or near 150°E.

Sea surface temperatures, in June and September 1981, are shows in the top pairs of panels in Fig. 2. As Occam includes no surface warming or cooling it is expected to show no seasonal changes and this is seen to be the case, Occam showing warmer temperatures in the southern hemisphere and cooler than Nemo in both June and September and cooler temperatures in the north. This is to be expected as Oceam lacks the surface heating in the northern summer and the cooling in the southern winter.

The sea level figures show better agreement. This is true for the large scale gyres of the north and south Pacific but, more importantly for this study, there is also good agreement in the development of the ridges and troughs on and just north of the Equator. Note, for example in the west equatorial Pacific, the height and extent of the maximum near the Equator and the depth and extent of the region of minimum sea level that develops just to the north-east of Mindinau. The differences are largest off Central America, where Occam fails to reproduce the East Pacific Warm Pool, and in the western section of the South Pacific, where there is little reduction of Occam temperatures between June and September. The regions of cold water, with temperatures at or below 20°C, also behave very differently in Occam and Nemo.

Along the line of the NECC at 6°N, Occam fails to show the warming during the first half of the year, but by September it does show a narrow band of warm water being advected into the eastern Pacific by the NECC. It also shows it being eroded by tropical instability eddies.

3.2 Comparison of 1982 results

The following six figures provide a similar set of comparisons for the classic Corresponding sets of panels for 1982, during the development of the 1982-1983 El Niño year of 1982. In this year both models show that, at 6°N, the drop in sea level in the western Pacific, associated with, are shown in Figs. 3, 4, 5 and 3.3.

In Fig. 3, Occam shows, in agreement with Nemo, a much deeper North Equatorial Trough in early June together with a well developed NECC. This is emphasised further in September with a deep trough in the west which extends almost as far as the Mindanao Eddy.

The Hovmöller diagrams of Fig. 5 show that in 1982 the arrival of the annual Rossby wave, is much stronger than in 1984 (a more normal year) in both Occam and Nemo, links with the region of low sea level that develops at the western end of the trough. Webb (2018b) argued that it was this drop which generated the increase the NECC strength which triggered the development of a classic oceanographic El Niño.

320 Similarly in Fig??, both models show At the Equator (Fig. 3.3), Occam shows, in agreement with Nemo, the movement of high sea levels into the central Pacific during the second half of the year, which again increased the strength of the NECC.

Figs. ?? to ??, compare surface temperatures and sea level during 1982. Again the temperature plots the maximum sea level away from the western boundary to a region near 200°E. In Figs. 3 and 4 this is seen to correspond to the region of high sea level on the equator where the warmest Equatorial temperatures are also found.

325 3.3 Summary of comparisons

The results show that the Occam is cooler in the northern hemisphere and warmer in the southern hemisphere.

The sea-level plots show that in both models show a similar extension of the North Pacific Trough towards the west and a similar weakening of both the Equatorial Trough and model is capturing the key features in the sea level field which affect the strength of the NECC, the strength of tropical instability waves. On the Equator they also show a similar movement of the 330 region of maximum sea level from the western Pacific to the central Pacific.

In conclusion, although the Occam model has only a third of the eddies and processes occurring on the Equator. It is less effective at capturing changes to sea surface temperature field. This may partly be due to the lack of surface heat fluxes in this version of the model. It may also be partly due to the much reduced horizontal resolution of the Nemo model, and although it is missing surface fluxes of heat and fresh water, it is capturing the key differences in sea level between the normal year of 335 1981 and the El Niño year of 1982. On this basis it can be usefully model.

However by bearing these strengths and weaknesses into account, there is no reason why it cannot be used to study the development of the ocean effect of the winds and the initial state of the ocean on the development of the 1982-1983 El Niño in more detail, as is done here.

(a)(b)

340 (a)(b)

Plots of Nemo model SST, SSH and surface velocities from the average over the 5 days before the 4th June 1981.

Plots of Occam model SST, SSH and surface velocities at the end of the 2nd September 1981.

Plots of Nemo model SST, SSH and surface velocities from the average over the 5 days before the 2nd September 1981.

345 (a)(b) Hoffmuller diagram the sea level at 6° N in the Pacific for 1982, showing (a) sea level from the Occam run and (b) from the Nemo run.

(a)(b) Hoffmuller diagram the sea level on the Equator in the Pacific for 1982, showing (a) sea level from the Occam run and (b) from the Nemo run.

Plots of Occam model SST, SSH and surface velocities at the end of the 4th June 1982.

Plots of Nemo model SST, SSH and surface velocities from the average over the 5 days before the 4th June 1982.

350 Plots of Occam model SST, SSH and surface velocities at the end of the 2nd September 1982.

Plots of Nemo model SST, SSH and surface velocities from the average over the 5 days before the 2nd September 1982.

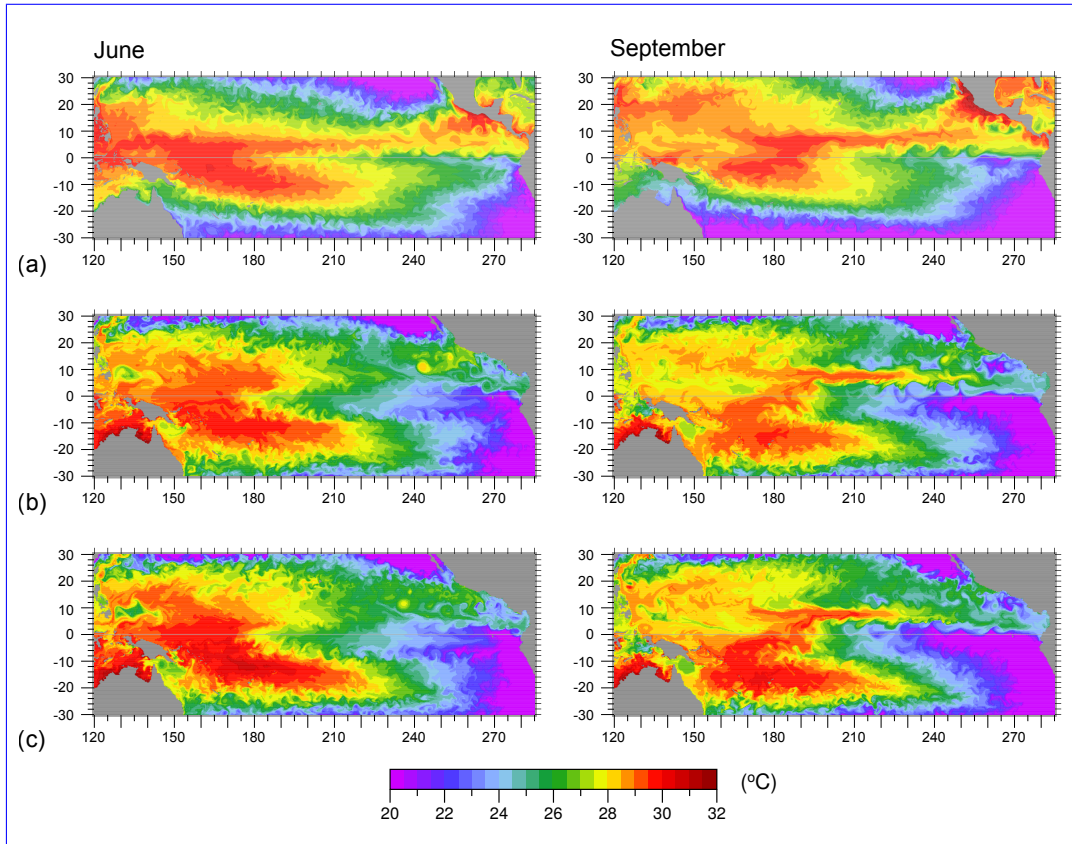


Figure 4. Hoffmuller diagram Surface temperature ($^{\circ}\text{C}$) on the 6th June and 9th September for (a) Nemo in 1982, (b) Occam in 1982, started January 1982 (c) Occam in 1981, started January 1981 but with 1982 winds.

4 Tests using wind stresses from different years

Although Webb (2018b) identified a number of processes contributing to the development of a strong El Niño in 1982 and 1997, the study was not able to explain why the events started in those years and not, say, a year earlier or a year later.

355 One possibility, suggested by Webb (2018b), is that there was something different about the stratification of the ocean in early 1982 and 1997, which focused the annual Rossby waves, so that they had a larger amplitude than usual once they reached the western Pacific. Another possibility is that the difference was due to the wind. This may have generated a stronger than normal annual Rossby wave that year. Alternatively some independent wind event may have occurred which lowered sea level in the western Pacific around the time that the leading edge of the annual Rossby wave arrived.

360 In an attempt to distinguish between these possibilities, the two Occam runs starting in January 1981 and 1982 were repeated, but this time forced by the winds from the opposite year. If focusing is important then then the January 1982 ocean, forced by the 1981 winds, might generate a similar enhanced annual Rossby wave in the western Pacific. Alternative in Alternatively if

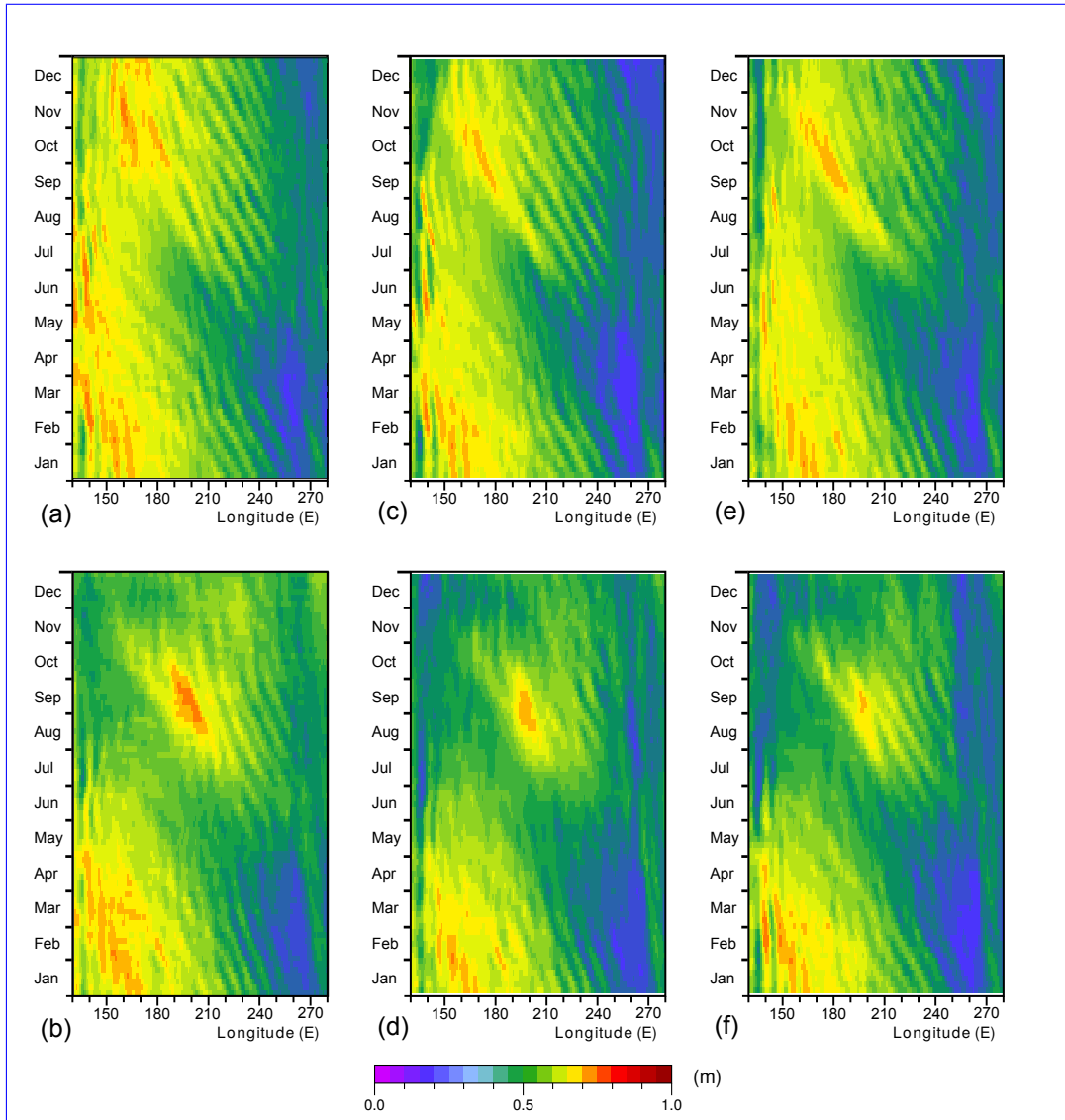
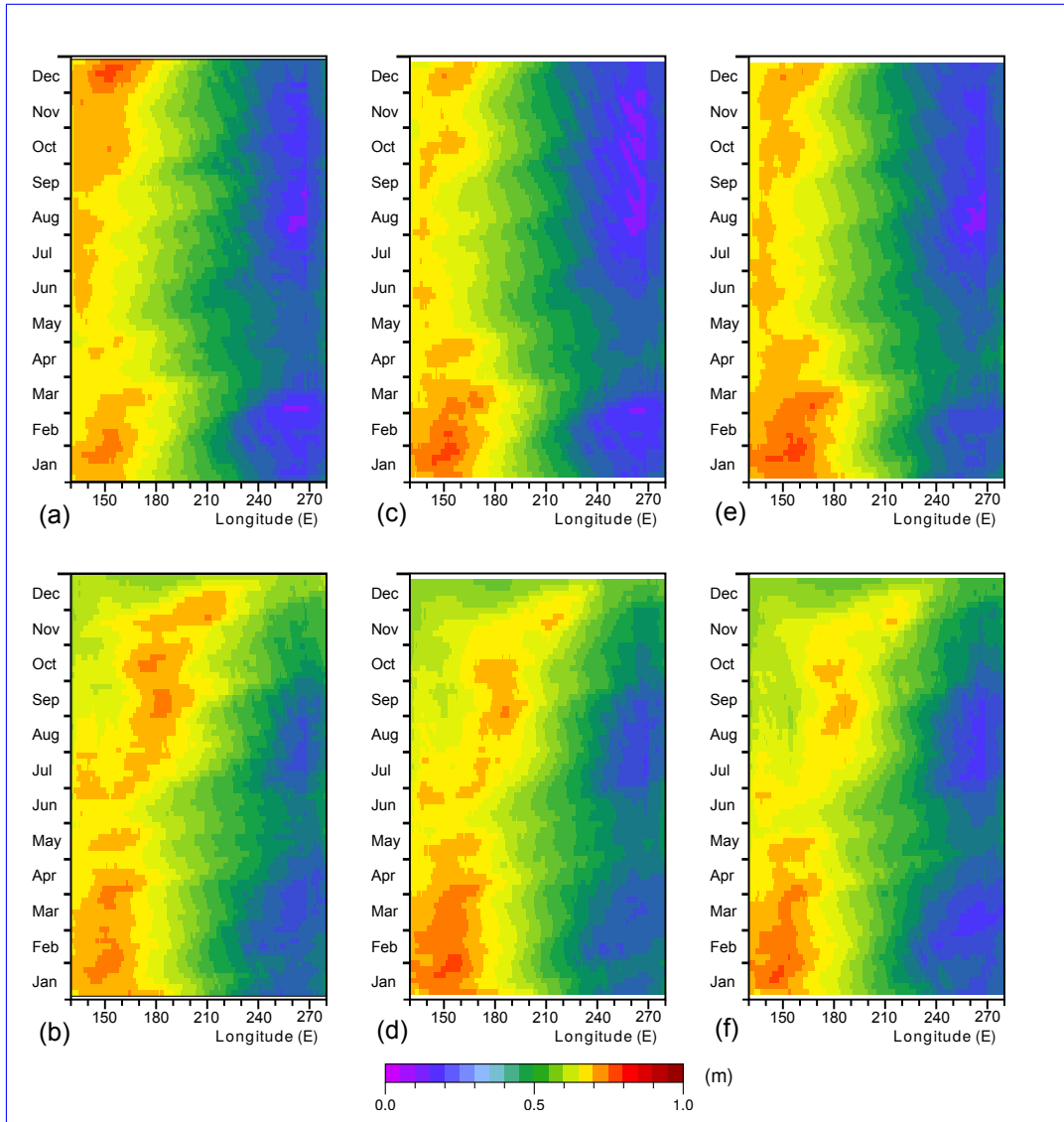


Figure 5. Hovmöller diagrams of sea level (m) at 6°N in the Pacific for 1981, showing (a) sea level from the short Occam 1/4° Nemo model run and in 1981, (b) from the Nemo 1/12° run in 1982, (c) Occam starting January 1981, (d) Occam starting January 1982, (e) Occam starting January 1982 but with 1981 winds, (f) Occam starting January 1981 but with 1982 winds. The figures are based on 1° averages of the model data.

the winds are important, then the January 1981 run, forced by the 1982 winds, ~~would~~ ~~might~~ generate the low sea level in the western Pacific.



Plots averages of Oceam model SST, SSH and surface velocities at the end of the 4th June 1981 model data.

Plots averages of Oceam model SST, SSH and surface velocities at the end of the 4th June 1981 model data.

Figure 6. Hoffmuller diagram—the Hovmöller diagrams of sea level (m) on the Equator in the Pacific for 1981, showing (a) sea level from the short Oceam 1/4° Nemo model and in 1981, (b) from the Nemo in 1982, (c) Occam starting January 1981, (d) Occam starting January 1982, (e) Occam starting January 1982 but with 1981 winds, (f) Occam starting January 1981 but with 1982 winds. The figures are based on 1/42° run.

Plots averages of Oceam model SST, SSH and surface velocities at the end of the 4th June 1981 model data.

365 4.1 January 1982 ocean forced by 1981 winds

In this test, the model was initialised from the Nemo archive dataset dated the 5th January 1982, but then forced with winds from 1981. Figure ?? (top) 5e shows how sea level developed at 6° N. ~~Here the N. During the first few months of the year the annual Rossby wave develops and propagates westwards as normal during the first few months of the year, but in mid-ocean the amplitude declines so by the time the wave reaches 180° E the signal is weak.~~

370 At the equator ~~On the Equator (Fig. 3.3e)~~, sea level starts high in the western Pacific, as in the previous run with 1982 winds (Fig. ??a, 3.3d), but as the year develops it stays in the west and there is no movement into the central Pacific.

Fig. ?? shows the surface temperature and sea level on the 4th June, a time when the transport by the NECC should start to increase. ~~The temperature field is comparable with the run with Figures 1c and 2c show the sea level and temperature fields for June and September. Previous runs with 1982 winds (Fig. ??) but the North Equatorial Trough is still only weakly developed and shows none of the westward extension expected for an El Niño year. show that by June the depth of the trough is starting to increase more than in a normal year but here this is not happening and instead the response is closer to that of Nemo in 1981. Similarly in September the trough fails to develop further and the response again lies closer to that of Nemo in 1981.~~

375 Fig. ?? is a similar plot from the autumn when the transport of warm water by the NECC would be large when an El Niño is developing. ~~The temperature figure does show a narrow band of warm water advected by the NECC but the area of warm water is much weaker than was generated with the 1982 winds (Fig. ??). Sea level has a similar problem, the North Equatorial Trough being much shallower than that generated with 1982 winds.~~

380 After mid-year, changes in the wind system due to the developing El Niño will normally reduce the strength of the Equatorial Current and result in less energetic tropical instability eddies. ~~Here because~~ The surface temperature field is also closer to the Nemo results from 1981 ~~winds are being used, some of the differences seen in autumn are to be expected even if a stronger NECC had been triggered in mid-year, with the bulk of the Warm Pool water remaining in the west. However there is a thin core of warmer NECC water extending into the eastern Pacific, which is not present in the run started in January 1981 with 1981 winds. This indicates that there was some change in the structure of the ocean between January 1981 and 1982 which aided the transport of warm water eastwards by the NECC.~~

390 ~~The~~ Despite this, the main conclusion from this run is that the ocean state at the start of 1982 was not sufficient to trigger an El Niño in mid-year. Although a reasonable annual Rossby wave was generated early in the year (Fig. ??), this was not focused and did not generate or contribute to the lowering of sea level in the western Pacific.

Plots of Oceam model SST, SSH and surface velocities at the end of the 2nd September 1982, of the run started from the Nemo archive of the 5th January 1982 but forced with 1981 winds.

395 Hoffmuller diagram the sea level from the Oceam model during 1981, when started from the Nemo model archive from the 5th January 1981 but forced by 1982 winds for (above) 6° N and (below) at the Equator. ~~Review version: Left and right when single column~~

Plots of Oceam model SST, SSH and surface velocities at the end of the 4th June 1981, of run started from Nemo model on 5th January 1981 but forced with 1982 winds.

(a)(b)Hoffmuller diagram the sea level from the Oceam model during 1982, when started from Nemo model archive for the 5th January 1982 but forced by 1981 winds for (above) 6° N and (below) at the Equator.

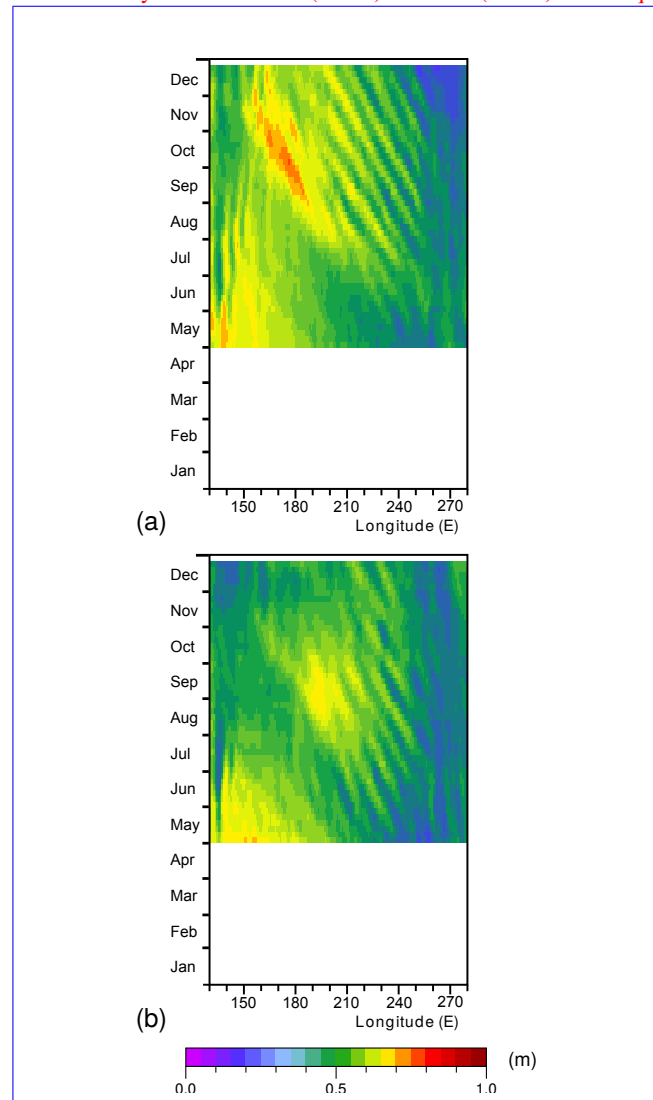


Figure 7. Plots Hovmöller diagram of Oceam model sea level (top) SST, at 6° N during 1982 for (bottom) SSH and surface velocities, at when started from the end of Nemo model archive from the 4th June–30th April 1982 but forced by 1981 winds, in the run (b) started from the Nemo model archive of from the 5th January 1982–30th April 1981 but forced with 1981 by 1982 winds.

Plots of Oceam model SST, SSH and surface velocities at the end of the 2nd September 1981, of run started from Nemo model on 5th January 1981 but forced with 1982 winds.

Hoffmuller diagram for the sea level at 6° N during 1982, when started from the Nemo model archive from the 30th April 1982 but forced by 1981 winds.

Hoffmuller diagram for the sea level at 6° N during 1981, when started from the Nemo model archive from the 30th April 1981 but forced by 1982 winds.

405 4.2 January 1981 ocean forced by 1982 winds

In the second test, the ocean is initialised from the Nemo archived dataset dated the 5th January 1981, but then forced with 1982 winds. Figure ?? (top) 5f shows the sea level during the year at 6° N. The annual Rossby starts as before, but this time it continues past 180° E and links up with a region of low sea level in the western Pacific - as might be expected in an at the start of a strong El Niño year.

410 On the Equator, Fig. ?? (bottom), (Fig. 3.3f) the ocean again starts with high sea levels in the west. In mid-year these move into the central Pacific - again as might be expected in an at the start of a strong El Niño year.

Figure ?? shows Figures 3c and 4c show that in mid-year the distribution of sea surface temperature is similar to the other Occam runs, but sea level shows a well developed North Equatorial Trough with a strong NECC developing on its southern slope.

415 By September (Fig. ??), the trough has developed further and the temperature plot shows warm surface water being advected rapidly into the eastern Pacific. The area of warm water involved is not as large as in the original Nemo run in 1982, but as with Fig. ?? 4b, this is probably a result of setting the surface flux of heat to zero in these test runs.

One conclusion from this test is that the ocean will produce an El Niño like response when forced by the winds from an El Niño year. This has been reported before, but based primarily on the large sea level and temperature anomalies that develop in 420 the western Pacific cold pool eastern Pacific Cold Pool towards the end of the first year of a classic oceanographic El Niño.

The cold pool is the region of cold water lying near the equator in the western Pacific which oceanographers associate with the upwelling of cold underecurrent water. During an El Niño, the easterly winds and underecurrent become weaker, less cold water is upwelled and as a result sea surface temperatures increase. This reduces the density of sea water, so sea level also rises.

425 The present case present study is different in that it shows the winds having a significant effect during the first half of the year, well before any changes in the atmospheric convection regime Cold Pool region are noticeable. The results also show that by mid-year the 1982 winds have produced significant changes in the western section of the North Equatorial Trough. What is not clear is whether , during this period, the increased depth of the North Equatorial Trough trough is due to a change in the mean winds during the period first part of the year or due to one or more isolated events.

430 It is also not clear whether it is due to a local change in the winds along the line of the Trough trough, or whether the key wind forcing occurs elsewhere and the signal propagates into the region lowering the level of the Trough trough. The remaining tests reported here are an attempt to obtain a clearer answer to these questions.

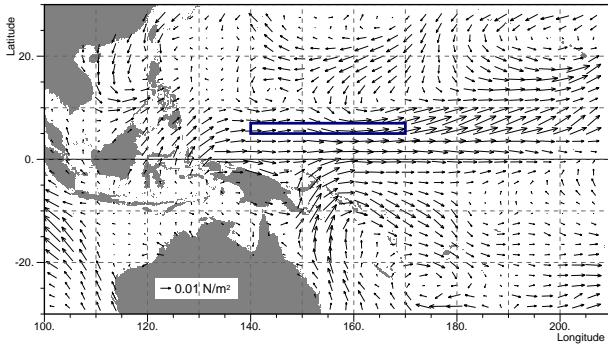


Figure 8. Wind stress vector anomaly (Nm^{-2}), for the period 16th March to the 8th August 1982 relative to the same period in 1981. The blue rectangle shows the region between 140°E and 170°E and between 5°N and 7°N .

5 Tests starting in late April

One possibility that has not been discounted is that ~~winds~~, early in the 1982, ~~the winds~~ generated a Rossby wave, or similar, 435 which was later responsible for the drop sea level drop in the western Pacific. To test this hypothesis, the model was started from ~~from~~ the Nemo archive dataset dated the 30th April 1982 and then forced with the 1981 winds. The start date is just before the start of the drop in sea level in the western Pacific. If the Rossby or other waves are responsible, then by that date they should be established enough to reproduce the drop in sea level despite the change in the wind field.

~~The result at 6°N is shown in Fig. 7. It shows that under these conditions a shows how sea level develops along 6°N . The annual Rossby wave starts propagating across the central Pacific as normal but near the dateline its amplitude is greatly reduced and there is no significant drop in sea level connection with the lower sea levels of the far western Pacific. Thus, although the test does not exclude events occurring before the 30th April having some impact, they can not be the prime cause of the sea level drop that increases the strength of the NECC near 160°E .~~

The complimentary test was also carried out, in which the ocean was started from the 30th April 1981 but forced with 1982 445 winds. The result, shown in Fig. ~~22~~7b, shows that sea level does drop. This implies that it is the winds after the 30th April 1982 that are responsible.

6 A Further Test with The role of local winds in the ~~Winds~~ western Pacific

Figure 8 shows the difference between the 1982 and 1981 wind stress vectors for the Pacific when averaged between the 16th March and the 8th August. It shows that in the western Pacific near the Equator, there is a significant westerly component to the wind stress anomaly. North of New Guinea this drops to zero near 10°N . This distance is typical of the atmospheric equatorial Rossby radius, a scale which also determines the northward extent of Madden-Julian Oscillations (~~MJOs~~)(Madden and Julian, 1971, 2012).

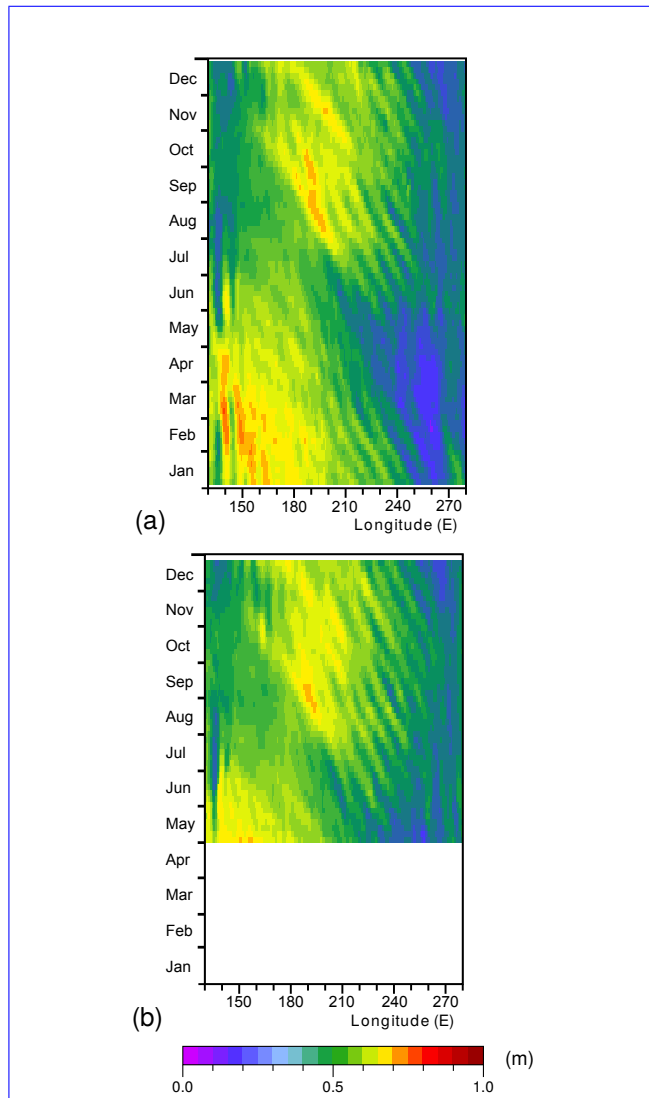


Figure 9. Hoffmuller-Hovmöller diagram for the ~~of~~ sea level (m) at 6°N during 1981, forced by the combination of 1981 and 1982 winds described in the main text when started from the NEMO archive for (above) 5th January 1981, (below) 30th April 1981. **Review version: Left and right.**

MJOs are reported to be stronger over the western Pacific prior to eastern Pacific El Niños (Chen et al., 2016). Thus the anomaly and the large north-south gradient in the wind stress may be ~~a result of~~ connected with the MJOs.

455 Further east the ITCZ often lies close to 10°N . It is not clear whether this is ~~also~~ related to the equatorial Rossby radius, but the figure shows that this is also ~~an~~ a region where both the wind stress anomaly and its north-south gradient ~~in the~~ can be large.

Table 1. Mean sea levels (m) between 140°E and 170°E and between 5°N and 7°N, at the end of April and August for the different runs, identified by the model and start month. The two groups correspond to runs forced by the 1981 winds and by either the 1982 winds or the combined winds.

		Start	Apr	Aug
81 Winds	Occam	Jan 81	0.620	0.557
	"	Jan 82	0.632	0.581
	"	Apr 81	0.633	0.520
	Nemo	Jan 81	0.605	0.570
82 Winds	Occam	Jan 82	0.582	0.341
	"	Jan 81	0.577	0.316
	"	Apr 81	0.672	0.356
	Nemo	Jan 81	0.559	0.364
Combined	Occam	Jan 81	0.590	0.354
	"	Apr 81	0.668	0.387

To see if the local wind fields in the western Pacific were responsible for the drop in sea level in 1982, a modified wind field was constructed which combined both the 1981 and 1982 winds. The weighting for the 1982 winds was defined so that it 460 ~~equaled~~ equalled one within the region between 140°E to 180°E and the Equator and to 15°N and was zero outside the region 130°E to 190°W and 10°S to 25°N. Linear interpolation was used between the two boundaries. Weighting for the 1981 field was set to one minus the 1982 weighting.

This results in the 1982 wind field being used for the area where the main sea level drop is observed and the 1981 wind fields being used elsewhere but with a smooth transition zone. The combined wind field was then used for two runs. As with 465 the previous tests using 1982 winds, the first started from the ocean state for the 3rd January 1981 and the second from the 30th April 1981. If the drop in sea level is due to local winds then the change in sea level should be similar to those obtained using only the 1982 wind field.

The resulting sea levels along 6°N are shown in Fig. 9. In both cases sea level starts dropping in the western Pacific in early May, confirming the importance of the local winds after the 30th April.

470 6.1 Intercomparison

Fig. 10 shows the changes in sea level from the different runs, averaged over the region 140°E to 170°E and 5°N to 7°N, as outlined in ~~fig~~ Fig. 8. The ~~ocean~~ Occam runs start with a slight offset from the corresponding runs of the Nemo model, due to the initial adjustment to the new coast and topography.

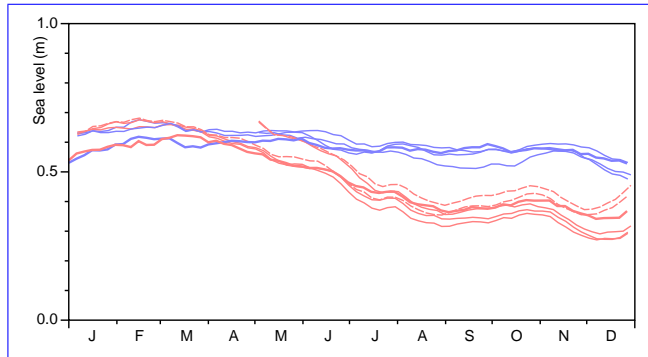


Figure 10. Sea level (m) in the different runs averaged between 140° -E and 170° -E and between 5° -N and 7° -N. Red Solid red lines correspond to runs forced by 1982 winds, blue to 1981 winds. Thick lines are from the original Nemo run, thin lines are from the [oceam-Occam](#) runs. The red dashed lines corresponds to the runs started in 1981 but with 1982 winds only in the western Pacific.

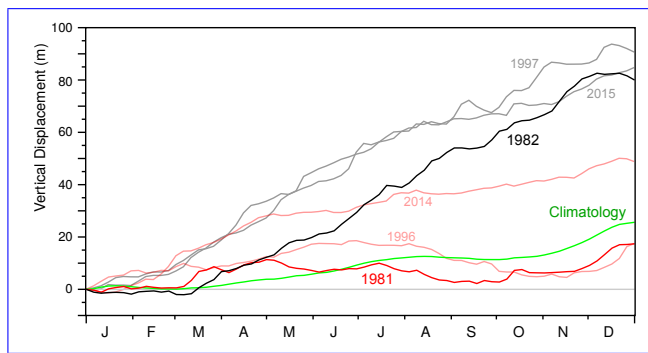


Figure 11. Integral over time of the vertical velocity due to Ekman divergence in the region bounded by 140° -E, 170° -E, 5° -N and 7° -N, during (black) 1982, (red) 1981, (green) climatology 1958-2015. [In the background are the corresponding plots for the years prior to the 1997-1998 and 2015-2016 El Niños.](#)

In this figure, colour is used to distinguish the different winds forcing the ocean, [red for 1982 and blue for 1981](#) and [red for 1982](#). Even with the different starting conditions, the runs soon split into two distinct groups, sea levels with the 1981 winds staying roughly constant whereas the 1982 winds generate a 20 cm drop between March and August. As pressures in the deep ocean remain roughly constant, this drop in sea level must correspond to a significant rise in the density surfaces within the ocean.

To quantify the differences between the groups, sea levels from the end of April and August are given in Table 1, split into runs forced by 1981 winds and those forced either by 1982 winds or by the combined wind fields. A t-test shows that the probability of both sets belonging to the same group at the end of April is around 0.5, as might be expected. By the end of August the probability drops to around 0.00002. A test using the sea level change over the period gives a similar value.

7 Winds and Ekman Divergence

Given that local winds appear to be responsible, the most likely cause of the rise in the density surfaces is that it is due to a
485 divergence in the wind generated Ekman transport in the surface layers of the ocean.

Here the possibility is investigated by calculating the Ekman pumping in the region 140°E to 170°E and 5°N to 7°N .

If the Ekman transport vector is $E(\theta, \phi)$, where θ and ϕ are latitude and longitude, then

$$E(\theta, \phi) = \tau(\theta, \phi) \times \hat{n} / (\rho f(\theta)) \quad (1)$$

where $\tau(\theta, \phi)$ is the wind stress vector, \hat{n} the unit vertical vector, ρ is the density and $f(\theta)$ is the Coriolis term, equal to,

$$490 \quad f(\theta) = 2 \Omega \sin(\theta). \quad (2)$$

Ω is the angular rotation rate of the Earth.

The averaged vertical velocity in a region, due the divergence of the Ekman flux, is then given by integrating the outward flowing Ekman transport around the region of interest,

$$P = -(1/A) \oint E(\theta; \phi) \wedge \hat{n} \cdot d\hat{s}, \quad (3)$$

$$495 \quad = (1/A) \oint \tau(\theta, \phi) \cdot d\hat{s} / (\rho f(\theta)). \quad (4)$$

where \hat{s} is the unit vector tangential to the boundary and A the area enclosed.

Fig. 11, shows the results obtained by integrating the vertical velocity over time. It shows that in 1982 the Ekman divergence (given by the slope of the curve) was positive for most of the period between April and late November, and that it had the potential for raising density surfaces within the ocean by 80 m. During the period mid-March to mid-August the potential rise
500 is approximately 50 m.

~~Nemo 1/12° model potential density during 1982, averaged between 140° E and 170° E and between 5° N and 7° N. Contours at integer values of density ().~~

A noticeable feature of ~~figs~~ [Figs.](#) 10 and 11 is that, during 1982, the drop in sea level and the vertical displacement due to the
505 Ekman divergence are both relatively steady processes ~~occurring~~ [occurring](#) over many months. There are short periods when the rate of change is reduced or reverses, but overall the results imply that the changes are a result of a long term systematic change in the wind field.

To check that the Ekman pumping is sufficient to cause the observed change in sea level, ~~figs. ?? and 12 show the~~ [Fig. 12 shows](#) density profiles from the original Nemo 1/12° model run averaged over the same area as before.

Figure [??](#) [12a](#) shows that during 1981, the changes in the depth of the density surfaces were small and at most depths had
510 balanced out by the end of the year.

In contrast, during 1982 (~~fig. 12~~ [Fig. 12b](#)), there was a significant shallowing of the density surfaces. The figure shows that in mid-March, water with densities of 1025 kg m^{-3} (approx 21.5°C) lay near 150 m, and that by mid-August it had risen to near 100 m. This rise of approximately 50 m is comparable with the Ekman pumping estimate. However after this period, although

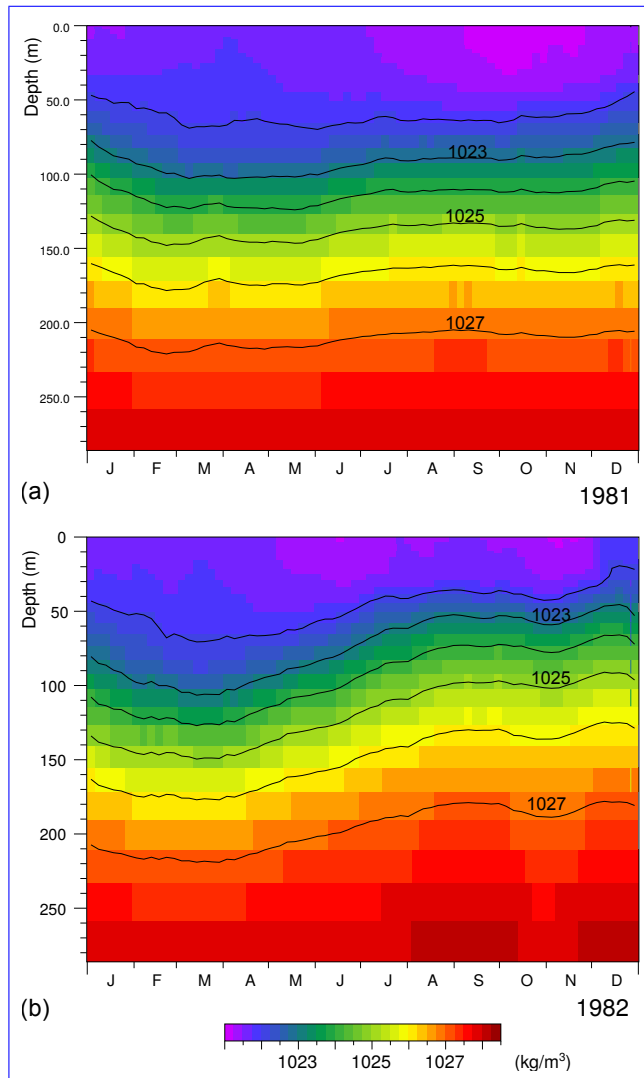


Figure 12. Nemo 1/12° model potential density during 1981, averaged between 140°-E and 170°-E and between 5°-N and 7°-N. Contours, interpolated from model layer values, for (a) 1981 and (b) 1982. Contours at integer values of density (kg m^{-3}).

the negative Ekman pumping continued there was no further shallowing in the density surfaces near the surface and there is
515 evidence of a rebound at depth.

7.1 The 1997-1998 and 2015-2016 El Niños

Figure 11 also shows the integrated Ekman pumping during the years prior to the strong EP El Niños of 1997-1998 and 2015-2016. In 1997 and 2015, the net vertical displacement was similar to the 1982 value but in both cases the Ekman pumping started earlier in the year.

520 The results also show that 1996 was not very different from climatology, but in 2014 the displacement curve starts by following the curves for 1997 and 2015 and it is only after April that the pumping is reduced. The displacement then continues to increases until the end of the year.

525 A number of papers, including Min et al. (2015), Chiodi and Harrison (2017) and Wang and Hendon (2017), suggest that an eastern Pacific El Niño started to develop in 2014 but was then prevented by a change in the winds. It is possible that the 2014 curve in Fig. 11 reflects this event.

530 The main conclusion to be taken from ~~these~~ ~~the~~ results is that ~~between~~ mid-March and mid-August ~~at the start of the 1982-1983 El Niño~~ ~~1982~~, there was a ~~strong~~ ~~large~~ amount of negative Ekman pumping (i.e. Ekman suction) in the western Pacific around 6° N due to a wind anomaly. ~~The results also indicate that this~~ ~~Similar amounts of Ekman pumping also occurred prior to the strong 1997-1998 and 2015-2016 El Niños. In each case the results indicate that the pumping~~ was due to a systematic change in the local wind field which lasted for many months.

535 Previously, ~~the papers by ? and Tan and Zhou (2018) both showed strong correlations~~ Hu et al. (2017) found a correlation between Ekman pumping north of the Equator and ~~the behaviour~~ cooling within the Warm Pool during an El Niño. Zhao et al. (2013) and Tan and Zhou (2018) described similar correlations with the strength of the NECC. However ~~the~~, given the processes and timings involved, the present results emphasise how the ~~changed NECC can then be~~ NECC can be part of an active trigger of strong El Niños rather than always representing a passive response to events elsewhere.

It thus seems likely that it is Ekman suction, due to the wind anomaly, which is responsible for the lower than normal sea level. To check that this is the case, Ekman suction is calculated for the region between 150° E to 170° E and 4° N and 10° N.

540 There is one complication in carrying out such a calculation near the Equator in that some of the north-south Ekman transport is compensated by a geostrophic flow associated with the wind induced pressure gradient along the equator. The combined effect, known as the tropical cell (Pujol et al., 2016), is a central part of Stommel's theory of the Pacific Undercurrent (Stommel, 1960; Webb, 2018a)).

Because of the relatively high speed of equatorial Kelvin waves, the pressure gradient along the Equator should closely follow the local eastward component of the wind stress. Assuming that this is true, and using Stommel's theory to correct for the tropical cell, E_n , the remaining northward component of Ekman transport is given by,

545
$$E_n(\theta, \phi) \equiv (\tau_e(\theta, \phi) - \tau_e(0, \phi)) / f(\theta),$$

where $\tau_e(\theta, \phi)$ is the eastward component of wind stress at latitude θ , longitude ϕ and $f(\theta)$ is the Coriolis term equal to,

$$f(\theta) \equiv = 2 \Omega \sin(\theta),$$

and Ω is the angular rotation rate of the earth.

550 Figure 11 shows the Ekman pumping integrated from the start of 1982 for the region 150° E to 170° E and 4° N to 8° N. The climatology curve shows that on average there is strong Ekman suction and for this reason the curves marked 1981 and 1982 are the integrals for those years relative to climatology.

They show that in 1981 the Ekman suction was smaller than normal between April and August and that in 1982 Ekman suction was stronger than usual during the same period and that this continued until late in the year, but at a reduced rate.

555 If no other processes were involved, the strong climatological Ekman suction would mean that this is a region of deep upwelling (in addition to the normal Equatorial Cell). However as this is not the case other processes must be involved. A likely candidate for this is a net poleward flow, as occurs in sub-polar oceanic gyres.

560 To see what actually happens, figs. ?? and 12 shows how the density profiles, also at 6° N averaged between 150° N and 170° N, develop during 1981 and 1982. Because the pressures deep in the ocean remain roughly constant, any movement of the density surfaces would be expected to be reflected in the change in sea level. Comparison with Fig 10 shows that this is the case.

Thus in 1981, the depth of the density surfaces oscillate slightly, but the net change over the year is small – as is yr chane in sea level. This confirms that the region is not one with deep upwelling. It also means that it may be possible to treat 1981 as a reference year, one where the total Ekman pumping roughly balances the otehr processes involved.

565 In 1982 the density surface rise steadily between March and August and this corresponds well with the drop in sea level of fig 10. It also corresponds with the extra Elman suction during this period seen in fig/ ??.

If 1981 is be trated as a reference year, and the other processes, referred to above, remain roughly constant then the differences in the integrated Elman pumping should correspond to the uplift of the density surfaces within the ocean.

The fact that the net changes in density and sea level during 1981 were small, indicates that it may be possible to treat this as a reference year.

570 Many studies of El Niños emphasise the role of equatorial Kelvin waves, generated by westerly wind burst along the Equator. Figure ?? shows the equatorial wind stress during 1982 using the same horizontal scale as Fig. 11. The peaks in the plot correspond to the features usually described as westerly wind bursts. Comparison with Fig. 11 shows that they are sometimes associated with increased Ekman suction at the latitudes of the North Equatorial Trough, but their net effect is minor, the steady lowering of sea level arising between March and August arising from the average increase in the eastward stress during this 575 period.

8 Conclusions

The primary aim of this study has been to understand the causes cause of the low sea levels that developed in the western Pacific, along the line of the North Equatorial Trough early in the development, during the growth of the strong 1982-1983 El Niño.

580 A comparison of results from the Nemo 1/12 degree° and Occam 1/4 degree° global ocean models indicated that that the latter was suitable for studying the development of the 1982-1983 El Niño in the Pacific.

The Occam model was then used in a series of short runs to determine which part of the whether the state of the ocean or the wind field was responsible for the low sea levels. The tests, in which the model was started from the ocean state at the beginning of 1981 and 1982 and forced by the winds from the opposite year, showed that the initial state of the ocean was not 585 critical, but that the model needed the 1982 winds in order to generate the sea level drop in the western pacific Pacific.

Similar tests, starting in mid-April, were used to check if Rossby or other waves, generated early each year, were important. However the ~~conclusion was results showed~~ that they had no significant effect.

In the final ~~set pair~~ of tests, the model was forced by 1981 winds everywhere except for a localised region in the western equatorial Pacific. ~~In both cases these runs of the model, where 1982 winds were used. Both runs~~ reproduced the drop in sea level ~~in the western Pacific~~, indicating that it was primarily the local winds, ~~acting around the same time as the drop in sea level~~, that were responsible.

A plot of the wind stress anomalies in 1982, showed that at latitudes between 5° N and 12° N in the western equatorial Pacific there ~~can be was~~ a significant gradient in the wind stress. Because of this, the amount of Ekman pumping was calculated. It was found that in 1981 the term was small, but that in 1982 significant Ekman pumping occurred between April and November. 595 The original Nemo model archive showed that from April onwards there was corresponding rise in the density surfaces, but that the rise stopped in August as the shallowest density surfaces neared the surface.

Allowing for this, the results indicate that the deepening of the North Equatorial Trough, between ~~130°~~ ~~140°~~ E and 170° E during the early development of the 1982-1983 El Niño, was due to Ekman suction caused by a period of anomalous surface wind stress.

600 North of New Guinea the anomalous wind stress has a structure similar to that expected from the westerly wind phase of a ~~Madden Julian~~ ~~Madden-Julian~~ Oscillation, with a maximum near the Equator and dropping to near zero at a latitude corresponding to the atmospheric Rossby radius. Further east the anomaly appears to be more connected to the shears associated with an active ~~intertropical convergence zone~~ ITCZ.

El Niños are often thought to be triggered by ~~Madden Julian~~ ~~Madden-Julian~~ Oscillations. Although not checked here it is 605 possible that in 1982 one or more MJOs were initially responsible for the westerlies that developed north of New Guinea. ~~The westerlies generated~~ ~~Westerlies would generate~~ an eastward flowing current along the Equator which ~~would have started moving the region of deep convection eastwards. There were also westerly wind bursts which generated equatorial Kelvin waves. , by transporting warm water, would have extended the region over which deep atmospheric convection could occur.~~

However acting over a period of months, the ~~westerlies winds~~ also increased the depth of the North Equatorial Trough 610 through Ekman pumping. ~~This~~ ~~As found in the NEMO model results (Webb, 2018b), this~~ increased the strength of the NECC, ~~which then carried more warm water eastwards than was normal. Further east strong wind shears developed, associated with the ITCZ, again with the potential of deepening the North Equatorial Trough and increasing the strength of the NECC water, warm enough to trigger deep atmospheric convection, into the eastern Pacific.~~

So in conclusion, a study of current and sea level changes in the ~~Equatorial Ocean~~ ~~equatorial Pacific, prior to the 1982-83 El Niño~~, has emphasised the role of the wind shears north of the Equator ~~and~~, the large amount of Ekman divergence that results, ~~and the potential core role of these processes in triggering strong EP El Niños.~~

~~In the western equatorial Pacific this increased the depth of the North Equatorial Trough and increased the transport of the North Equatorial Counter Current. As discussed in Webb (2018b) this was timed to connect with the increased transport due to the annual Rossby wave and so caused the strong El Niño of 1982-1983.~~

620 At a more general level, this study has also emphasised the mismatch between the ocean's equatorial Rossby radius, the scale of the ocean's tropical cell and the much large scale of the atmosphere's equatorial Rossby radius. Without this mismatch the North Equatorial Trough would probably not be so deep and the NECC ~~would~~ could not have had such an important role in the development of the 1982-1983 El Niño.

625 *Code and data availability.* At the time of publication the Nemo model datasets are freely available at "<http://gws-access.ceda.ac.uk/public/nemo/runs/OR06/means/>". The Nemo ocean model code and its documentation are available from "<http://forge.ipsl.jussieu.fr/nemo/wiki/Users>". The Occam model is based on the Moma ocean model available from "<https://github.com/djwebb/moma>".

Author contributions. The author is responsible both the model runs and the analysis.

630 *Acknowledgements.* This work contributed to and was aided by the research programme of the Marine Systems Modelling group at the UK National Oceanography Centre ([NOC](#)), part of the Natural Environment Research Council ~~.The Natural Environment Research Council~~ ([NERC](#)). [NERC](#) helped fund the investigation through the NOC National Capability funding. Part of the analysis was carried out using the JASMIN Service at the UK Centre for Environmental Data Analysis, also funded by NERC.

[The author also wishes to acknowledge the helpful comments and suggestions from Harry Bryden, D. Wang and three anonymous reviewers.](#)

References

635 Ashok, K., Behera, S. K., Rao, S. A., Weng, H., and Yamagata, T.: El Niño Modoki and its possible teleconnection, *Journal of Geophysical Research*, 112, <https://doi.org/10.1029/2006JC003798>, 2007.

Baturin, N. and Niiler, P.: Effects of instability waves in the mixed layer of the equatorial Pacific, *Journal of Geophysical Research*, 102, 27,771–27,793, 1997.

Bjerknes, J.: Atmospheric Teleconnections from the Equatorial Pacific, *Monthly Weather Review*, 97, 163–172, 1969.

640 Bryan, K.: A numerical method for the study of the circulation of the world ocean, *Journal of Computational Physics*, 4, 1255–1273, 1969.

Bryden, H. L. and Brady, E. C.: Diagnostic Model of the Three-Dimensional Circulation in the Upper Equatorial Pacific Ocean, *Journal of Physical Oceanography*, 15, 1255–1273, 1985.

Byrne, M. P., Pendergrass, A. G., Rapp, A. D., and Wodzicki, K. R.: Response of the Intertropical Convergence Zone to Climate Change: Location, Width, and Strength, *Current Climate Change Reports*, 4, 355–370, <https://doi.org/10.1007/s40641-018-0110-5>, 2018.

645 Cane, M. A.: Oceanographic Events during El Niño, *Science*, 222, 1189–1195, 2011.

Chelton, D. B., Wentz, F. J., Genremann, C. L., de Szoeke, R. A., and Schlax, M. G.: Satellite Microwave SST Observations of Transequatorial Tropical Instability Waves, *Geophysical Research Letters*, 27, 1239–1242, 2000.

Chen, X., Ling, J., and Li, C.: Evolution of the Madden–Julian Oscillation in Two Types of El Niño, *Journal of Climate*, 29, 1919–1934, 2016.

650 Chiodi, A. M. and Harrison, D. E.: Observed El Niño SSTA Development and the Effects of Easterly and Westerly Wind Events in 2014/15, *Journal of Climate*, 30, 1505–1519, 2017.

Clarke, A. J.: El Niño Physics and El Niño Predictability, in: *Annual review of Marine Science*, vol. 6, pp. 79–99, Annual Reviews, 2014.

Cox, M.: A primitive equation 3-dimensional model of the ocean, Ocean Group Technical Report 1, Geophysical Fluid Dynamics Laboratory, Princeton University, Princeton, N.J. 08542, 1989.

655 de Cuevas, B., Webb, D., Coward, A., Richmond, C., and Rourke, E.: The UK Ocean Circulation and Climate Advanced Modelling Project (OCCAM), in: *High Performance Computing*, edited by Allan, R., Guest, M., Simpson, A., Henty, D., and Nicole, D., pp. 325–336, Kluwer Academic, New York, 681 pp., 1999.

Dussin, R., Barnier, B., Brodeau, L., and Molines, J. M.: The making of Drakkar forcing set DFS5, Report DRAKKAR/MyOcean Report 01-04-16, Laboratoire de Glaciologie et Géophysique de l'Environnement CNRS, Université de Grenoble, 2016.

660 Evans, J. L. and Webster, C. C.: A variable sea surface temperature threshold for tropical convection, *Australian Meteorological and Oceanographic Journal*, 64, S1–S8, <https://doi.org/10.22499/2.6401.007>, 2014.

Flato, G., Marotzke, J., Abiodun, B., Braconnot, P., Chou, S., Collins, W., Cox, P., Driouech, F., Emori, S., Eyring, V., Forest, C., Gleckler, P., Guilyardi, E., Jakob, C., Kattsov, V., Reason, C., and Rummukainen, M.: Climate Change 2013: The Physical Science Basis. Contribution of Working Group I to the Fifth Assessment Report of the Intergovernmental Panel on Climate Change, chap. Evaluation of Climate Models, Cambridge University Press, Cambridge, United Kingdom and New York, NY, USA, 2013.

665 Gadgil, S., Joseph, P. V., and Joshi, N. V.: Ocean-atmosphere coupling over monsoon regions, *Nature*, 312, 141–143, 1984.

Griffies, S. M., Gnanadesikan, A., Dixon, K. W., Dunne, J. P., Gerdes, R., Harrison, M. J., Rosati, A., Russell, J. L., Samuels, B. L., Spelman, M. J., Winton, M., and Zhang, R.: Formulation of an ocean model for global climate simulations, *Ocean Science*, 1, 45–79, 2005.

Guilyardi, E., Wittenberg, A., Fedorov, A., Collins, M., Wang, C., Capotondi, A., and van Oldenborg, G. J.: Understanding El Niño in
670 Ocean–Atmosphere General Circulation Models: Progress and Challenges, *Bulletin of the American Meteorological Society*, 90, 325–340, 2009.

Ham, Y.-G. and Kug, J.-S.: How well do current climate models simulate two types of El Niño?, *Climate Dynamics*, 39, 383–398, 2012.

Hansen, D. V. and Paul, C. A.: Genesis and Effects of Long waves in the Equatorial Pacific, *Journal of Geophysical Research*, 89, 10,431–10,440, 1984.

675 Hsin, Y.-C. and Qiu, B.: Seasonal fluctuations of the surface North Equatorial Countercurrent (NECC) across the Pacific basin, *Journal of Geophysical Research*, 117, 1–17, <https://doi.org/10.1029/2011JC007794>, 2012.

Hsu, C.-W., Yin, J., Griffies, S. M., and Dussin, R.: A mechanistic analysis of tropical Pacific dynamic sea level in GFDL-OM4 under OMIP-I and OMIP-II forcings, *Geoscientific Model Development*, 14, 2471–2502, <https://doi.org/10.5194/gmd-14-2471-2021>, 2021.

Hu, S., Hu, D., Guan, C., Xing, N., Li, J., and Feng, J.: Variability of the western Pacific warm pool structure associated with El Niño,
680 *Climate Dynamics*, 49, 2431–2449, <https://doi.org/10.1007/s00382-016-3459-y>, 2017.

Hurlburt, H., Kindle, J. C., and O'Brien, J. J.: A Numerical Simulaiton of the Onset of El Niño, *Journal of Physical Oceanography*, 6, 621–631, 1976.

Jochum, M., Cronin, M. F., Kessler, W. S., and Shea, D.: Observed horizontal temperature advection by tropical instability waves, *Geophysical Research Letters*, 34, 1–4, 2007.

685 Johnson, G. C., Sloyan, B. M., Kessler, W. S., and McTaggart, K. E.: Direct measurements of upper ocean currents and water properties across the tropical Pacific during the 1990s, *Progress in Oceanography*, 52, 31–61, 2002.

Kashino, Y., Atmadipoera, A., Kuroda, Y., and Lukijanto: Observed features of the Halmahera and Mindanao Eddies, *Journal of Geophysical Research Oceans*, 118, 6543–6560, <https://doi.org/10.1002/2013JC009207>, 2003.

Kennan, S. C. and Lament, P. J. F.: Observations of a Tropical Instability Vortex, *Journal of Physical Oceanography*, 30, 2277–2301, 2000.

690 Knauss, J. A.: The Structure of the Pacific Equatorial Countercurrent, *Journal of Geophysical Research*, 66, 143–155, 1961.

Larkin, N. K. and Harrison, D. E.: On the definition of El Niño and associated seasonal average U.S. weather anomalies, *Geophysical Research Letters*, 32, <https://doi.org/10.1029/2005GL022738>, 2005.

Lengaigne, M., Boulanger, J.-P. H., Menkes, C., Masson, S., Madec, G., and Delecluse, P.: Ocean response to the March 1997 Westerly Wind Event., *Journal of Geophysical Research*, 107, 8015–, <https://doi.org/1029/2001JC000841>, 2002.

695 Love, C.: EASTROPIC Atlas Vol 1, Government Printing Office, Washington, D.C., 1972.

Love, C.: EASTROPIC Atlas Vol 9, Government Printing Office, Washington, D.C., 1975.

Madden, R. A. and Julian, P. R.: Description of a 40–50 day oscillation in the zonal wind in the tropical Pacific, *Journal of Atmospheric Science*, 28, 702–708, 1971.

Madden, R. A. and Julian, P. R.: Description of global-scale circulation cells in the tropics with a 40–50 day period, *Journal of Atmospheric
700 Science*, 29, 1109–1123, 1972.

Madden, R. A. and Julian, P. R.: Historical perspective, in: *Intraseasonal Variability in the Atmosphere–Ocean Climate System (Second Edition)*, edited by Lau, W. K. M. and Waliser, D. E., pp. 1–16, Springer, 2012.

Madec, G., amd M. Imbard, P. D., and Lévy, C.: OPA 8.1 Ocean General Circulation Model reference manual, Note du Pole de modelisation XX, Institut Pierre-Simon Laplace (IPSL), France, 1998.

705 McCreary, J.: Eastern Tropical response to Changing Wind Systems: with applicaiton to El Niño, *Journal of Physical Oceanography*, 6, 632–645, 1976.

McCreary, J. P.: Modelling Equatorial Ocean Circulation, *Annual Review of Fluid Mechanics*, 17, 359–409, 1985.

McPhaden, M. J.: Continuously Stratified Models of the Steady-State Equatorial Ocean, *Journal of Physical Oceanography*, 11, 337–354, 1981.

710 McPhaden, M. J.: Trade Wind Fetch Related Variations in Equatorial Undercurrent Depth, Speed, and Transport, *Journal of Geophysical Research*, 98, 2555–2559, 1993.

Menkes, C., Vialard, J., Kennan, S., Boulanger, J.-P., and Madec, G.: A Modeling Study of the Impact of Tropical Instability Waves on the Heat Budget of the Eastern Equatorial Pacific, *Journal of Physical Oceanography*, 36, 847–865, 2006.

Min, Q., Su, J., Zhang, R., and Rong, X.: What hindered the El Niño pattern in 2014, *Geophysical Research Letters*, 42, 6762–6770, 2015.

715 Montgomery, R. and Palmen, E.: Contribution to the question of the Equatorial Counter Current, *Journal of Marine Research*, 4, 112, 1940.

Munk, W. H.: On the wind driven ocean circulation, *Journal of Meteorology*, 7, 79–93, 1950.

Myers, G.: On the Annual Rossby Wave in the Tropical North Pacific Ocean, *Journal of Physical Oceanography*, 9, 663–674, 1979.

Myers, G. and Donguy, J.-R.: The North Equatorial Countercurrent and heat storage in the western Pacific Ocean during 1982–83, *Nature*, 312, 258–268, 1984.

720 Neumann, G. and Pierson, W. J.: *Principals of Physical Oceanography*, Prentice-Hall, Inc., 1966.

Pacanowski, R. and Philander, S.: Parameterization of vertical mixing in numerical models of tropical oceans, *Journal of Physical Oceanography*, 11, 1443–1451, 1981.

Philander, S.: El Niño and La Niña, *Journal of Atmospheric Sciences*, 42, 2652–2662, 1985.

Philander, S.: El Niño and La Niña, *American Scientist*, 77, 451–459, 1989.

725 Picaut, J., Ioualalen, M., Menkes, C., Delcroix, T., and McPhaden, M. J.: Mechanism of the Zonal Displacements of the Pacific Warm Pool: Implications for ENSO, *Science*, 274, 1486–1489, <https://doi.org/10.1126/science.274.5292.1486>, 1996.

Pujol, M.-I., Faugère, Y., Taburet, G., Dupuy, S., Pelloquin, C., Ablain, M., and Picot, N.: DUCS DT2014: then new multi-mission altimeter data set reprocessed over 20 years, *Ocean Science*, 12, 1067–2016, <https://doi.org/10.5194/os-12-1067-2016>, 2016.

Semtner, A.: A general circulation model for the World Ocean, Technical Report No. 9, Department of Meteorology, University of California, 730 Los Angeles, 1974.

Smith, R., Dukowicz, J., and Malone, R.: Parallel ocean general circulation modelling, *Physica D*, 60, 39–61, 1992.

Stommel, H.: Wind-drift near the Equator, *Deep Sea Research*, 6, 298–302, [https://doi.org/10.1016/0146-6313\(59\)90088-7](https://doi.org/10.1016/0146-6313(59)90088-7), 1960.

Sun, Z., Liu, H., Lin, P., Tseng, Y., Small, J., and Bryan, F.: The Modeling of the North Equatorial Countercurrent in the Community Earth System Model and its Oceanic Component, *Journal of Advances in Modelling Earth Systems*, 1, 531–544, 735 <https://doi.org/10.1029/2018MS001521>, 2019.

Sverdrup, H. U.: Wind-driven currents in a baroclinic ocean; with application to the equatorial currents of the eastern Pacific, *Proceedings of the National Academy of Sciences*, 33, 318–326, 1947.

Taft, B. and Kovala, B.: Vertical sections of temperature, salinity, thermosteric anomaly and zonal geostrophic velocity from NORPAX Shuttle Experiment – Part 1., NOAA Data Report PMEL-10, PMEL, 1981.

740 Taft, B. and Kovala, B.: Vertical sections of temperature, salinity, thermosteric anomaly and zonal geostrophic velocity from NORPAX Shuttle Experiment – Part 3., NOAA Data Report ERL PMEL-7, PMEL, 1982.

Tan, S. and Zhou, H.: The observed impacts of the two types of El Niño on the North Equatorial Countercurrent in the Pacific Ocean, *Geophysical Research Letters*, 45, 10,439–10,500, <https://doi.org/10.1029/2018GL079273>, 2018.

Thompson, S. D.: Sills of the Global Ocean: a compilation, https://www.nodc.noaa.gov/woce/woce_v3/wocedata_2/bathymetry/sills/index.htm, 1996.

745 Wang, G. and Hendon, H. H.: Why 2015 was a strong El Niño and 2014 was not, *Geophysical Research Letters*, 44, 8567–8575, <https://doi.org/10.1002/2017GL074244>, 2017.

Webb, D.: The vertical advection of momentum in Bryan-Cox-Semtner ocean general circulation models, *Journal of Physical Oceanography*, 25, 3186–3195, 1995.

750 Webb, D., Coward, A., de Cuevas, B., and Gwilliam, C.: A Multiprocessor Ocean General Circulation Model Using Message Passing, *Journal of Atmospheric and Oceanic Technology*, 14, 175–183, [https://doi.org/10.1175/1520-0426\(1997\)014<0175:AMOGCM>2.0.CO;2](https://doi.org/10.1175/1520-0426(1997)014<0175:AMOGCM>2.0.CO;2), 1997.

Webb, D., de Cuevas, B., and Richmond, C.: Improved advection schemes for ocean models, *Journal of Atmospheric and Oceanic Technology*, 15, 1171–1187, 1998.

755 Webb, D. J.: A comparison of sea surface temperatures in the Equatorial Pacific Niño regions with results from two early runs of the NEMO 1/12° Ocean Model, *Research and Consultancy Report*, No. 55, National Oceanography Centre, Southampton, U.K., <http://nora.nerc.ac.uk/id/eprint/513264>, 2016.

Webb, D. J.: A Note on Stommel's Theory of the Tropical Cell, *Research and Consultancy Report*, No. 63, National Oceanography Centre, Southampton, U.K., <http://nora.nerc.ac.uk/id/eprint/520018>, 2018a.

760 Webb, D. J.: On the role of the North Equatorial Current during a strong El Niño, *Ocean Science*, 14, 633–660, <https://doi.org/10.5195/os-14-633-2018>, 2018b.

Webb, D. J., Coward, A. C., and Snaith, H. M.: A comparison of ocean model data and satellite observations of features affecting the growth of the North Equatorial Counter Current during the strong 1997–1998 El Niño, *Ocean Science*, 16, 565–574, <https://doi.org/10.5195/os-16-565-2020>, 2020.

765 Wijaya, Y. J. and Hisaki, Y.: Differences in the Reaction of North Equatorial Countercurrent to the Developing and Mature Phase of ENSO Events in the Western Pacific Ocean, *Climate*, 9, 175–183, <https://doi.org/10.3390/cli9040057>, 2021.

Wyrski, K.: Teleconnections in the Equatorial Pacific Ocean, *Science*, 180(4081), 66–68, 1973.

770 Wyrski, K.: Equatorial Currents in the Pacific 1950 to 1970 and Their Relation to the Trade Winds, *Journal of Physical Oceanography*, 4, 372–380, 1974a.

Wyrski, K.: Sea Level and the Seasonal Fluctuations of the Equatorial Currents in the Western Pacific Ocean, *Journal of Physical Oceanography*, 4, 91–103, 1974b.

775 Wyrski, K. and Kilonsky, B.: Mean Water and Current Structure during the Hawaii-to-Tahiti Shuttle Experiment, *Journal of Physical Oceanography*, 14, 242–254, 1984.

Wyrski, K., Stroup, E., Patzert, W., Williams, R., and Quinn, W.: Predicting and Observing El Niño, *Science*, 191, 343–346, 1976.

Yu, J.-Y. and Liu, W. T.: A linear relationship between ENSO intensity and tropical instability wave activity in the eastern Pacific Ocean, *Geophysical Research Letters*, 30, CLM 5–1 – 5–5, <https://doi.org/10.1029/2003GL017176>, 2003.

780 Yu, Z., McCreary, J. P., Kessler, W. S., and Kelly, K. A.: Influence of Equatorial Dynamics on the Pacific North Equatorial Countercurrent, *Journal of Physical Oceanography*, 30, 3179–3190, 2000.

Zhang, C.: Large-Scale Variability of Atmospheric Deep Convection in Relation to Sea Surface Temperature in the Tropics, *Journal of Climate*, 6, 1898–1913, 1993.

Zhang, C.: Madden-Julian Oscillation, *Reviews of Geophysics*, 43, 1–36, <https://doi.org/10.1029/2004RG000158>, 2005.

Zhang, R.-H. and Busalacchi, A. J.: A Possible Link between Off-equatorial Warm Anomalies Propagating along the NECC Path and the Onset of the 1997-98 El Niño, *Geophysical Research Letters*, 26, 2873–2876, 1999.

Zhao, J., Li, Y., and Wang, F.: Dynamical responses of the west Pacific North Equatorial Countercurrent (NECC) system to El Niño events, *Journal of Geophysical Research: Oceans*, 118, 2828–2844, <https://doi.org/10.1002/jgrc.20196>, 2013.